



Effect of Plant Material and Plant Density on Growth and Yield Performances of Srivijaya Pineapple [*Ananas comosus* (L) Merr.] under Intercropping with Young Oil Palm

Valentina, L.¹, Seephueak, P.¹, Boonchareon, K.² Chotikamas, T.³, Vanichpakorn, P.¹ and Sriporaya, S.^{1*}

¹ Agricultural Science Division Faculty of Agriculture Rajamangala University of Technology Srivijaya, Nakhon Si Thammarat, 80240

² Science Division Faculty of Science and Technology Rajamangala University of Technology Srivijaya, Nakhon Si Thammarat, 80240

³ Rubber Authority of Thailand, Surat Thani, 84210

* Corresponding author: suneerat.s@rmutsv.ac.th

Abstract

The research aim to determine the suitable plant density and plant material of the Srivijaya pineapple under intercropping with young oil palm. The result showed that Srivijaya pineapple had big challenges of waterlogging during the rainy season. Srivijaya pineapple at plant density 21,687 plants per hectare reached 18 cm plant height and plant material from 2.0 mg/L BA gave the highest plant height. The widest plant width was 90.31 cm using 1.0 mg/L BA followed by 89.10 cm using 2.0 mg/L BA. The total fruit weight at plant density 21,687 plants per hectare gave higher total fruit weight (679.29 grams), fruit weight (612.93 grams) and smaller core (2.30 cm). Plant material used 1.5 mg/L BA gave the highest average of total fruit (695.42 grams) and 629.05 grams for average fruit weight. TSS of plant materials from 1.5 mg/L BA was 17.89 °Brix. The yield production was 14.73 tons per hectare at a density of 21,687 plants per hectare which higher 2.86 tons compared to plant density 19,275 plants per hectare. Plant material sourced from 1.5 mg/L BA was the highest yield which reached 14.30 tones. Srivijaya pineapple production decreased 39 to 45.2% due to the waterlogging. Planting materials from tissue culture were 99% free disease on the growth stage of pineapple and had less than 12% of disease severity on post-growth stage.

Keywords: intercropping plant density, plant material, Srivijaya pineapple

Introduction

Pineapple (*Ananas comosus* (L.) Merr.) is an important tropical plant widely grown commercial tropical fruit in the world (Carlier *et al.*, 2007). Srivijaya hybrid pineapple having good quality and disease resistance such as heart rot, and root rot as well as wilt diseases was bred by Sriporaya (2009). The fruit quality characters; antioxidant activity 88.52 %, protein 4.84 %, fiber 3.86 % and bromelain 6,332.85 mg/ml were reported (Department of Agriculture, 2021). Freshly ripened pineapple fruit contains bromelain, it is useful for anti-inflammatory reasons and lowering swelling in inflammatory diseases (Hossain *et al.*, 2015).

There is open space in the field for intercropping crops during oil palm under 4 years. Farmers were obliged to spend their money on other agricultural tasks like weeding even though they had no income yet



(Tonye *et al.*, 2004). According to Valentina *et al.* (2023), Srivijaya pineapple is a suitable and profitable intercrop with young oil palm (Krualee *et al.*, 2021). Moreover, cultivation management is a prime factor for pineapple plantations. Plant density and plant material were the keys to gain high production and fruit quality. However, BA application on tissue culture may affect growth, and suckers in pineapples and it may affect yield (Valentina *et al.*, 2023).

In addition, environmental factors are necessary for optimal growth and yield. Srivijaya pineapple plants were sensitive to some conditions, for instance flooding and waterlogging. Waterlogging has an impact on insufficient supply of oxygen. Root respiration becomes less extensive so that the absorption of nutrients needed by the plant is inhibited. Prolonged water logging conditions and poorly aerated soils induce stress on the plants and reduce yield (Haque *et al.*, 2020). Therefore, it is critical to determine the best plant density and plant material for growth and yield on the Srivijaya variety production intercropping with young oil palm.

Materials and Methods

The experiment was conducted in a one-year oil palm field in Thung Yai district, Nakhon Si Thammarat Province, Thailand. It is a hills area with coordinates 8°17'48"N 99°22'30"E 500 meters above sea level (Wikipedia, 2023). The plant material was 'Srivijaya' pineapple plantlets from tissue culture propagation. Srivijaya pineapple plant materials were fed with MS+BA 1.0 mg/L, MS+BA 1.5 mg/L, and MS+BA 2.0 mg/L in tissue culture system. 'Srivijaya' pineapple plantlets were moved to a greenhouse and media containing soil, coconut peat, and rice husk charcoal in a ratio of 1:1:1. Plant materials were healthy and uniform based on age (one year) and plant height size (30 cm). A nine-meter triangular oil palm planting pattern was used. The pineapple planting pattern was used in the double and triple rows for the field experiment. A double row of 50 cm x 50 cm x 100 cm was used for 19,275 plants per hectare, and a triple row of 50 cm x 50 cm x 50 cm x 100 cm, for 21,687 plants per hectare. NPK 15-15-15 and NPK 0-0-60 were used to fertilize pineapple plants for growth and fruit, respectively. 15 grams per plant NPK fertilizer were applied per plant per fertilize period. 200 grams per plant of chicken manure were applied 4 months after planting. Herbicide used to suppress weeds at 3, 6, and 8 months after planting. Pineapple plants were watering automatically by an irrigation system powered by solar cells if there was no rain.

Experimental research design

This research used a split plot design in a randomized complete block with four replications. The main-plot was plant density having two densities; 19,275 and 21,687 plants per hectare. The sub-plot was plant materials sourced from plantlets that were produced by tissue culture using MS medium in three different BA concentrations (1.0 mg/L, 1.5 mg/L, and 2.0 mg/L). It used 200 and 300 plantlets per treatment for 19,275 and 21,687 plant densities, respectively. Ten plants per treatment in each replication were sampled for data recording. The variables growth data measured were D-leaf length and width, plant height and plant width, average of new suckers and slip. Diseases data including heart rot, root rot and wilt disease. Yield data including total fruit weight, fruit weight, crown weight, fruit width and length, core width, eye depth and TSS (total soluble solid). Data on D-

leaf length and width was recorded using a caliper and a ruler from the most recently longest and widest leaf of pineapple. Yield data for weight used balance and for length and width used ruler. TSS used refractometer. Heart rot and root rot were identified by the leaf color changes to yellow; stunted growth and death. Wilt disease was identified by wilt in the leaves of pineapple; the leaf color changes to orange from the tip part, and the leaf texture is soft. Data was collected and analyzed using analysis of variance (ANOVA). The Duncan Multiple Range Test was used for the mean difference analysis at 5 % and 1 % levels.

Results and Discussion

Pineapple plants were grown under intercropping with young oil palms. However, it faced the problem of waterlogging during the rainy season and it decreased the growth performance of Srivijaya pineapple.

D-leaf length and D-leaf width of Srivijaya pineapple

Plant density and plant material gave no significant impact on d-leaf length and increasing D-leaf length. The average D-leaf length was higher at denser densities of Srivijaya pineapple than 19,275 plants/ha (Table 1). Plant material from the tissue culture system using 2.0 mg/L BA was also the longest D-leaf per 3 weeks observed. The D-leaf width was higher at a higher plant density (21,687 plants/ha) than 19,275 plants/ha. Plantlets from tissue culture using 2.0 mg/L BA gave the longest D-leaf width every 3 weeks. Data showed that the pineapple's D-leaf width increased less than 1 cm after three weeks and six weeks of fertilizing at 31 WAP (Table 2). This study was agreed by Hotegni (2014) who reported that the highest proportion of heterogeneity in fruit weight was explained by the number of functional leaves (NL) × D-Leaf, which is best related to leaf areas.

Table 1 Effect of plant density and plant material on D-leaf length of Srivijaya pineapple at 31-37 WAP in Thung Yai district

Factors	D-leaf length (cm)			Increasing D-leaf length (cm)	
	31 WAP	34 WAP	37 WAP	34 WAP	37 WAP
Plant density (D)					
19,275 plants/ha	36.18	37.26	38.25	1.08	0.99
21,687 plants/ha	38.49	39.82	40.80	1.32	0.99
Plant material					
1.0 mg/L BA	36.26	37.46	38.45	1.20	0.99
1.5 mg/L BA	36.45	37.62	38.55	1.17	0.93
2.0 mg/L BA	39.30	40.53	41.58	1.23	1.05
D	ns	ns	ns	ns	ns
M	ns	ns	ns	ns	ns
D X M	ns	ns	ns	ns	ns
CV (%)	10.43	10.97	10.23	70.76	38.86

ns = no significant according to Duncan's multiple range test, p<0.05

Table 2 Effect of plant density and plant material on D-leaf width of Srivijaya pineapple at 31-37 WAP in Thung Yai district

Factors	D-leaf width (cm)			Increasing D-leaf width (cm)	
	31 WAP	34 WAP	37 WAP	34 WAP	37 WAP
Plant density (D)					
19,275 plants/ha	2.35	2.40	2.47	0.053	0.065
21,687 plants/ha	2.53	2.59	2.69	0.062	0.100
Plant material (M)					
1.0 mg/L	2.48	2.54	2.63	0.060	0.100
1.5 mg/L	2.34	2.39	2.47	0.055	0.074
2.0 mg/L	2.50	2.56	2.64	0.058	0.074
D	ns	ns	ns	ns	ns
M	ns	ns	ns	ns	ns
D X M	*	*	ns	ns	ns
CV (%)	12.23	11.79	11.82	61.59	63.36

ns = no significant; *significant at $p \leq 0.05$; means in the same column followed by the same letter were not significantly different according to Duncan's multiple range test, $p < 0.05$

Plant height and increasing of plant height Srivijaya pineapple

The study reveals that the plant height of Srivijaya pineapples reached 15.70 cm to 18.83 cm after one year after planting (Table 3). The highest plant height was observed with plant material containing 2.0 mg/L BA and 1.0 mg/L BA at every time of data collection. The increase in plant height reached 7 cm to 9 cm after 49 weeks after planting (Table 4). The pineapple plant's stem performance is evident, with rapidly expanding leaves providing a natural shield for fruits, reducing evaporative loss, producing shade, and preventing weed growth Assumi *et al.* (2021). The plant height was higher in higher density, with plant density with 21,687 plants/ha resulting in 18.04 cm, or 2.59 cm higher than pineapple grown with 19,275 plants/ha.

Table 3 Effect of plant density and plant material on plant height of Srivijaya pineapple at 31-49 WAP in Thung Yai district

Factors	Plant height (cm)						
	31 WAP	34 WAP	37 WAP	40 WAP	43 WAP	46 WAP	49 WAP
Plant density (D)							
19,275 plants/ha	8.91	9.92	11.70	12.87	14.09	15.49	16.23
21,687 plants/ha	9.82	11.58	13.22	14.47	15.87	17.83	18.82
Plant material (M)							
1.0 mg/L	9.78 ^a	11.16 ^a	13.08 ^a	14.45 ^a	15.54 ^a	17.24 ^a	18.04 ^a
1.5 mg/L	8.13 ^b	9.44 ^b	10.88 ^b	11.88 ^b	13.05 ^b	14.96 ^b	15.70 ^b
2.0 mg/L	10.19 ^a	11.64 ^a	13.43 ^a	14.68 ^a	16.35 ^a	17.79 ^a	18.83 ^a
D	ns						
M	**	**	**	**	**	*	*
D X M	ns						
CV (%)	15.65	17.23	16.77	17.44	16.31	14.78	15.70

ns = no significant; *significant at $p \leq 0.05$; **significant at $p \leq 0.01$; means in the same column followed by the same letter were not significantly different according to Duncan's multiple range test, $p < 0.05$

Table 4 Effect of plant density and plant material on increasing of plant height of Srivijaya pineapple at 34-49 WAP in Thung Yai district

Factors	Increasing of plant height (cm)						
	34 WAP	37 WAP	40 WAP	43 WAP	46 WAP	49 WAP	Total
Plant density (D)							
19,275 plants/ha	1.01	1.78	1.17	1.23	1.40	0.73	7.32
21,687 plants/ha	1.76	1.64	1.25	1.40	1.97	0.98	9.00
Plant material (M)							
1.0 mg/L	1.39	1.91	1.38	1.09	1.70	0.80	7.58
1.5 mg/L	1.31	1.44	1.00	1.18	1.91	0.74	8.26
2.0 mg/L	1.45	1.79	1.25	1.68	1.44	1.04	8.64
D	ns	ns	ns	ns	ns	ns	ns
M	ns	ns	ns	ns	ns	ns	ns
D X M	ns	ns	ns	ns	ns	ns	ns
CV (%)	35.45	27.72	35.19	44.79	28.15	28.53	21.85

ns = no significant according to Duncan's multiple range test, $p < 0.05$

Plant width and increasing of plant width of Srivijaya pineapple

Compared to plant material sourced by BA concentrations, 1.0 mg/L BA was the best to support plant width growth following 2.0 mg/L BA and giving 90.31 cm and 89.10 cm respectively a year after planting (Table 5). Both different plant density and plant material did not significantly impact the increasing plant width. Growth of Srivijaya pineapple was sluggish throughout the 49 WAP of increasing plant height (Table 6). This was consistent with the sigmoid curve, which shows that early growth goes slowly. The plant density has no discernible effect on the pineapple's width. One of the many advantages of high-density planting is the overlapping of the basal leaves, which produces shade and reduces evaporative loss as well as weed growth. As a result of the high plant density, the quickly expanding leaves tended to twist and grow straight, providing the fruits with a natural shield from sunburn and resulting in glossy, uniformly colored fruits (Assumi *et al.*, 2021).

Table 5 Effect of plant density and plant material on plant width of Srivijaya pineapple at 31-49 WAP in Thung Yai district

Factors	Plant width (cm)						
	31 WAP	34 WAP	37 WAP	40 WAP	43 WAP	46 WAP	49 WAP
Plant density (D)							
19,275 plants/ha	69.42	72.62	75.75	77.87	80.75	83.97	85.81
21,687 plants/ha	75.23	79.01	81.61	83.73	85.33	88.17	90.51
Plant material (M)							
1.0 mg/L	75.23 ^a	78.73 ^a	81.23 ^a	82.75a	84.68 ^a	88.29 ^a	90.31 ^a
1.5 mg/L	67.33 ^b	70.86 ^b	74.59 ^b	77.33b	80.15 ^b	83.05 ^b	85.06 ^b
2.0 mg/L	74.43 ^a	77.85 ^a	80.23 ^a	82.31a	84.30 ^a	86.86 ^{ab}	89.10 ^a
D	ns	ns	ns	ns	ns	ns	ns
M	*	*	*	*	ns	*	*
D X M	ns	ns	ns	ns	ns	ns	ns
CV (%)	12.10	11.41	9.30	8.87	7.04	6.45	6.18

ns = no significant; *significant at $p \leq 0.05$; means in the same column followed by the same letter were not significantly different according to Duncan's multiple range test, $p < 0.05$

Table 6 Effect of plant density and plant material on increasing of plant width of Srivijaya pineapple at 34-49 WAP in Thung Yai district, Nakhon Si Thammarat

Factors	Increasing of plant width (cm)						Total
	34 WAP	37 WAP	40 WAP	43 WAP	46 WAP	49 WAP	
Plant density (D)							
19,275 plants/ha	3.20	3.13	2.12	2.88	3.22	1.84	16.39
21,687 plants/ha	3.78	2.60	2.12	1.61	2.83	2.34	15.28
Plant material (M)							
1.0 mg/L	3.50	2.50	1.53	1.93	3.61	2.03	15.09
1.5 mg/L	3.54	3.73	2.74	2.83	2.90	2.01	17.74
2.0 mg/L	3.43	2.38	2.09	1.99	2.56	2.24	14.68
D	ns	ns	ns	ns	ns	ns	ns
M	ns	ns	ns	ns	ns	ns	ns
D X M	ns	ns	ns	ns	ns	ns	ns
CV (%)	31.26	45.63	40.47	46.64	23.27	29.53	36.19

ns = no significant according to Duncan's multiple range test, $p < 0.05$

Average of new suckers and slips of Srivijaya pineapple plants

Plant density and material factors significantly influence the total number of suckers in Srivijaya pineapple plants (Table 7). Higher plant density (21,687 plants/ha) led to more suckers than 19,275 plants/ha during the growing period. Plant material also had a significant impact on suckers. The growth stage showed the most significant increase in suckers, with BA 2 mg/L producing 0.94 suckers at 49 WAP. Growth regulators (BA) in tissue culture regulate stem elongation and apical dominance, and many suckers develop when pineapple is replanted in the field. Higher plant density and higher BA concentrations induce more suckers in pineapple plants, potentially due to larger plants in an area. It was confirmed that the effect of higher BA from tissue culture induced more new shoots until the cultivation on field (Valentina *et al.*, 2020). Excessive suckers before flowering can impact the quantity and quality of fruit. Zhang *et al.* (2016) found that tissue culture plant material produced 7.75 suckers, larger than 0.75 suckers from sucker material. Tissue culture systems and growth regulators help produce a large number of shoots, but excessive suckers before fruit is ready to flower can decrease fruit diameter due to the sharing of nutrients between pineapple and suckers (Markos, 2014; Valentina *et al.*, 2019). New suckers continue to grow slowly in the growth stage, with an average of 1-2 suckers after the flowering phase. The average slip in the growth phase was less than one sucker per plant. Normally, commercial pineapple varieties such as Phuket or Pattavia varieties have no slip. Slips also occur more at the pineapple plant growth period. Srivijaya pineapple variety showed an average less than one slip which was a performance that is a suitable trait.

Table 7 Effect of plant density and plant material on average of new suckers of Srivijaya pineapple in Thung Yai district

Factors	Average of new suckers (sucker)								
	Week after planting	Before flowering						After flowering	
		31	34	37	40	43	46	49	
Plant density (D)									
19,275 plants/ha	0.04	0.15 ^b	0.20 ^b	0.22 ^b	0.40 ^b	0.44 ^b	0.53	1.88	
21,687 plants/ha	0.09	0.24 ^a	0.35 ^a	0.43 ^a	0.65 ^a	0.69 ^a	0.78	1.60	
Plant material (M)									
1.0 mg/L	0.06	0.15 ^b	0.18 ^b	0.23 ^b	0.36 ^c	0.43 ^b	0.49	2.18	
1.5 mg/L	0.04	0.14 ^b	0.22 ^b	0.25 ^b	0.41 ^b	0.43 ^b	0.55	1.47	
2.0 mg/L	0.11	0.30 ^a	0.43 ^a	0.51 ^a	0.82 ^a	0.84 ^a	0.94	1.58	
D	ns	*	*	*	*	*	ns	ns	
M	ns	*	*	*	*	*	ns	ns	
D X M	ns	ns	ns	ns	ns	ns	ns	ns	

ns = no significant; *significant at $p \leq 0.05$; means in the same column followed by the same letter were not significantly different according to Duncan's multiple range test, $p < 0.05$

The yield of Srivijaya pineapple affected by plant material and plant density

Srivijaya pineapple plant includes the fruit shown in Figure 2. The average of total fruit weight from planting density 21,687 plants per hectare was 679.29 grams which was 63 grams more than from 19,275 plants per hectare (Table 8). It demonstrated that the total fruit weight did not decrease when planting density was increased at higher density. Plant material fed by 1.5 mg/l BA was the biggest fruit giving 695.42 grams although was not significant. The result was agreed with previous reports that pineapple fruit quality characteristics were not significantly impacted by planting density. The fruit weight of Srivijaya pineapple was less than the common characteristics of Srivijaya which reached 1.120 kilograms per fruit (Sripaoraya *et al.*, 2023). Although the size of the fruits was reduced, higher planting densities boosted the overall fruit output (Assumi *et al.*, 2021). The width of the pineapple core, fruit diameter, fruit height, fruit weight, ripening period, and harvest duration all had a positive correlation with pineapple yield. It implies that the pineapple's core width increases as yield rises. In addition, the fruit's diameter, height, weight, ripening period, and harvest period all lengthen (Wiangsamut, and Koolpluksee, 2018).

The small crown of Srivijaya pineapple was less than 100 grams and ranging between 60 to 66 grams. The average crown weight per plant on single factor was used in 21,687 plants per hectare (57.65 grams), plant material fed by 1.0 mg/L BA (53.33 grams) gave effect on smaller crowns. Plant density, plant material and interaction had no significant effect on the core of Srivijaya pineapple. The core of Srivijaya pineapple was a variety in the range of 2.2 to 2.4 cm. The core of Srivijaya pineapple on single factor was used in 21,687 plants per

hectare (2.30 cm), using plant material 2 mg/L BA (2.31 cm) gave smaller core. The eye depth in 19,275 plants per hectare gave 0.74 cm and plant material BA 2 mg/L gave 0.82 cm which showed smaller eye depth than others.

Average of TSS at 19,275 plants/ha (17.99°Brix) was higher than at 21,687 plants/ha (17.40°Brix). Plant material 1.5 mg/L BA (17.89 cm) gave higher TSS although no significantly different effect. It showed that both in higher density or different plant material can be used depending on which one can improve the production. This study found that the sweetness level of Srivijaya pineapple under intercropping with young oil palm gave close TSS performance to Srivijaya pineapple that had TSS 17.80 °Brix (Sripaoraya *et al.*, 2023). According to the Department of Agriculture (2021), Srivijaya pineapple fruit has 17.80 °Brix. This study found the average of TSS was 17.40-17.99°Brix. The Srivijaya pineapple has a sweet taste similar to the previous report of Department of Agriculture (2021). This study found that TSS of Srivijaya pineapple was higher than the parent materials, Phuket variety was 16°Brix (Chainark *et al.*, 2018) and Pattavia was 12.6°Brix (Chuenboonngarm *et al.*, 2007). Compared to another cultivar, the total soluble solids content of Srivijaya pineapple was higher than *Ananas comosus* L. Merr. cv. Sarawak which has 12.7 °Brix (George *et al.*, 2016).

The study found that planting density and yield had a direct proportional relationship. Yield rose as the number of plants per unit area increased. Yield production was 14.73 tons per hectare at a density of 21,687 plants per hectare was 2.68 tons higher compared to 19,275 plants/ha. Plant material sourced from 1.5 mg/L BA was the highest yield reaching 14.30 tones. It means that a higher BA (2.0 mg/L BA) did not mean a higher yield. Srivijaya pineapple production decreased 39 to 45.2% compared to common production due to the waterlogging. Stress from waterlogging has a negative impact on vegetative and reproductive growth, which can result in harvest failure or yield loss (Pan *et al.*, 2021).

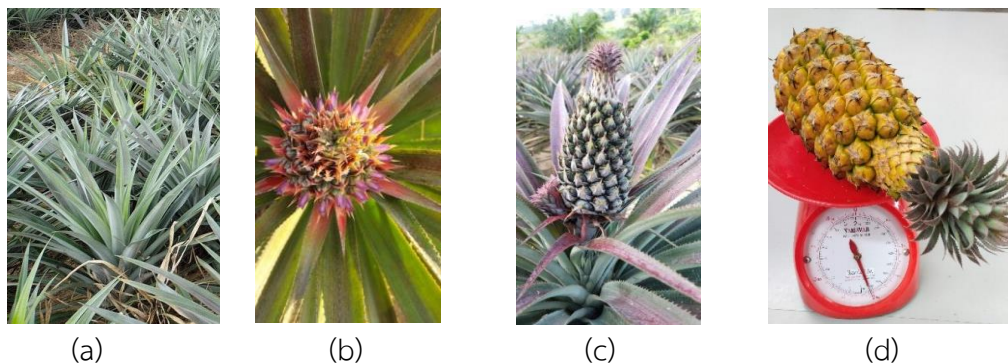


Figure 2. Srivijaya pineapple (a) leaves (b) flower (c) fruit (d) ripe fruit

Table 8 Effect of plant density and plant material on yield and production of Srivijaya pineapple in Thung Yai district

Factors	Yield and production								
	Fruit weight total (g)	Fruit weight (g)	Crown weight (g)	Fruit width (cm)	Fruit length (cm)	Core width (cm)	Eye depth (cm)	TSS (°Brix)	Production (ton)
Plant density (D)									
19,275 plants/ha	615.80	558.15	57.65	9.44	11.57	2.38	0.74	17.99	11.87
21,687 plants/ha	679.29	612.93	66.37	9.59	11.19	2.30	1.47	17.40	14.73
Plant material (M)									
1.0 mg/L BA	603.08	549.76	53.33	9.35	11.95	2.38	1.61	17.57	12.36
1.5 mg/L BA	695.42	629.05	66.37	9.78	10.88	2.33	0.88	17.89	14.30
2.0 mg/L BA	644.14	583.53	60.61	9.43	11.31	2.31	0.82	17.63	13.24
D	ns	ns	ns	ns	ns	ns	ns	ns	ns
M	ns	ns	ns	ns	ns	ns	ns	ns	ns
D X M	ns	ns	ns	ns	**	ns	ns	ns	ns
CV (%)	17.34	18.74	44.22	7.37	14.04	11.81	132.20	10.35	17.34

ns = no significant; **significant at $p \leq 0.01$; means in the same column followed by the same letter were not significantly different according to Duncan's multiple range test, $p < 0.05$

Disease of Srivijaya pineapple

The study found that Srivijaya pineapple plants were completely free of disease from 28 WAP to 46 WAP, with only 0.13% cases of heart rot, 0% cases of root rot, and 0% cases of wilt disease during the growth stage. This indicates that heart rot, root rot, and wilt diseases are not harmful to 99.87% of the plants. This is consistent with previous research by Jackson *et al.* (2016) and Valentina *et al.* (2023), which found that clean plant materials produced by tissue culture systems. However, at 49 WAP, only 0.13% and 0.06% of heart rot and Phytophthora cases were infected, indicating a 99% resilience of the plants to these diseases. This result is similar to study from Valentina *et al.* (2023) showed 100% resistance to diseases at the growth phase of Srivijaya pineapple. Wilt disease in Srivijaya pineapple increased during the post-harvest phase, with a higher incidence at planting density of 21,687 plants per hectare compared to 7.9% at planting density of 19,275 plants per hectare. The study found that Srivijaya pineapple is resistant to wilt disease, with disease severity being less than 12%. Waterlogging conditions in the soil can lead to adverse effects on Pythium and Phytophthora root rot. Plant growth and productivity are affected by their sensitivity to waterlogging, and in extreme cases, plants may even die (Dayalan *et al.*, 2021). The disease severity in the harvesting phase was higher than in the growth phase, but the increase in



disease diversity was still low at less than 9%, indicating that Srivijaya pineapple is classified as a strong variety. The factor contributing to increased wilt disease is the larger colony of mealybugs, which grow quickly when pineapple plants have fruit (Dey *et al.*, 2018).

Conclusions

Srivijaya pineapples have grown under intercropping with young oil palm and estimated yield higher three tons at 21,687 plants/ha compared to plant density (19,275 plants/ha). Plant materials from micro-propagation fed by 1.5 mg/L BA was the highest yield by producing an estimated 14.30 tons per hectare. Srivijaya pineapple was sensitive to waterlogging and it decreased production compared to original characteristics of Srivijaya pineapple. Srivijaya pineapples were more than 99% resistant to disease in growth phase and disease severity was less than 12% or lightly disease category on post-growth.

Acknowledgements

The authors are thankful to Faculty of Agriculture, Rajamangala University of Technology Srivijaya and Thailand Science Research and Innovation Foundation for supporting research.

References

- Assumi S. R., Singh, P. T., and Jha A. K. 2021. Pineapple (*Ananas comosus* L. Merr.). In SN Ghosh, S. N., and R. R. Sharma (Eds.), Tropical fruit crops: theory to practical. pp 487-541. Jaya Publishing House.
- Carlier, J. D., d'Eeckenbrugge, G. C., and Leitao, J. M. 2007. Pineapple. In Kole, C (Eds.), Fruits and nuts: genome mapping and molecular breeding in plants. pp. 331-342. Springer
- Chainark, S., Jariyalperong, P. and Phetchaiya, T. 2018. The Relationship between Soil Properties and Climate on Quality of Geographical Indication "Phuket Pineapple" (*Ananas comosus*). Academic Conference and Innovation, Educational Innovation, Issues and International, Chiang Mai, Thailand, 2018, May 17-18
- Chuenboongarm, N., Juntawong, N., Engkagul, A., Arirob, W., and Peyachoknakul, S. 2007. Changing in TSS, TA and sugar contents and sucrose synthase activity in ethephon-treated 'pattavia' pineapple fruit. Kasetart Journal - Natural Science 41(2): 205-212.
- Dayalan, D.M., Kumar, R. A., Senthilkumar, S., Srivignesh, S., and Manivannan, S. 2021. Impacts of flooding stress in fruit crops and its adaptation strategies. *Ricerca International Journal of Multidisciplinary Research and Innovation* 2(3): 1-6.
- Department of Agriculture. 2021. Plant Varieties Protection Office. Available from: https://www.doa.go.th/pvp/wppcontent/uploads/2021/06/AnnoDOA_PublicNo.146.pdf [accessed on 20 June 2024].
- Dey, K.K., Green, J.C., Melzer, M., Borth, W. and Hu, J.S. 2018. Mealybug wilt of pineapple and associated viruses. *Horticulturae* 4(52).

- George, D., Razali, Z., & Somasundram, C. (2016). Physical and physiochemical changes that occurs during growth and development of the Sarawak pineapple (*Ananas comosus* L. Merr. Cv Sarawak). *Journal of Agricultural Science and Technology* 18: 491-503
- Haque, S., Akbar, D. and Kinnear, S. 2020. The variable impacts of extreme weather events on fruit production in subtropical Australia, *Scientia Horticulturae*, 262.
- Hossain, M. F., Shaheen A., and Anwar, M. 2015. Nutritional value and medical benefits of pineapple. *International Journal of Nutrition and Foods Sciences* 4(1): 84-88.
- Hotegni, V. N. 2014. Using agronomic tools to improve pineapple quality and its uniformity in Benin. M.Sc. Master thesis. Wageningen University.
- Jackson, D., Williams, S., Newby, D., Hall, S., Higgins, S., Francis, R. and Smith, A. 2016. Tissue cultured versus traditionally grown pineapples: growth and nutrient profile. *Journal of Biotechnology and Biomaterials* 6(3): 1-5.
- Krualee, S., Sripeam, S., Chuchert, S., and Puttakan, T. 2021. Effect of Intercropping on growth and profit of oil palm in immature Stage. *Songklanakarin Journal of Plant Science* 8(2): (73-78).
- Markos, D. 2014. Effect of mulch type, ground cover percentage and sucker management in growth and yield of pineapple (*Ananas comosus* L.Merril.) under growing conditions of Sidama Zone, Southern Ethiopia. *Journal of Biology, Agriculture and Healthcare* 4(6): 27-32.
- Valentina, L., Seephueak, P., Boonchareon, K., Chotikamas, T., Vanichpakorn, P., and Sriporaya, S. 2023. Effect of planting materials and fertilizers on pineapple (*Ananas comosus* var. srivijaya) growth under intercropping with young oil palm (*Elaeis guineensis* Jacq. 1st International Conference on Science and Technology, Yala, Thailand, February 21-22 2023.
- Pan, J., Sharif, R., Xu, X. and Chen, X. 2021. Mechanisms of waterlogging tolerance in plants: research progress and prospects. *Frontiers in Plant Science* 11
- Sriporaya, S. 2009. Pineapple hybridization and selection in Thailand. *Acta Horticulturae* 822: 57-62.
- Sriporaya, S., Valentina, L., Vanichpakorn, P., Seephueak, P., Boonchareon, K. and Chotikamas, T. 2023. Efficiency for shoot multiplication of “Srivijaya” new hybrid pineapple variety using three tissue culture systems. *Thai journal of science and technology* 11(4): 64-74.
- Tonye, J., Bayomock, L. A., and Zoa J. M. 2004. Development of oil palm-based agroforest at the slash-and-burn agriculture project zone of Cameroon: agronomy and economics of the establishment phase. *Cameroon Journal Agricultural Science* 1(1): 42–45.
- Wiangsamut, B., and Koolpluksee, M. 2018. Effect of various ethephon concentrations on flowering, yield, costs and returns of productions of four pineapple varieties. *International Journal of Agricultural Technology* 14(7): 2215-2228
- Wikipedia. Thung Yai District. Available from https://en.wikipedia.org/wiki/Thung_Yai_district. [accessed on 20 June 2024].



Identification of *Cannabis* strains using the Inter-Simple Sequence Repeats (ISSR) Molecular Marker

Keomany, S.¹, Wongdee, J.², Greetatorn, T.², Songwatana, P.², Piromyou P.², Umnajkitikorn, K.³, Tittabutr, P.¹, Tantasawat, P.³, Teamtaisong, K.⁴, Boonkerd, N.¹ and Teaumroong, N.^{1*}

¹Suranaree University of Technology, School of Biotechnology, Institute of Agricultural Technology, 111 University Avenue, Muang, Nakhon Ratchasima 30000

²Institute of Research and Development, Suranaree University of Technology, 111 University Avenue, Muang, Nakhon Ratchasima 30000

³Suranaree University of Technology, School of Crop Production Technology, Institute of Agricultural Technology, 111 University Avenue, Muang, Nakhon Ratchasima 30000

⁴The Center for Scientific and Technological Equipment, Suranaree University of Technology, 111 University Avenue, Muang, Nakhon Ratchasima 30000

*Corresponding author: neung@sut.ac.th

Abstract

Cannabis is plant in the Cannabaceae family, and is generally divided into two categories: marijuana and hemp. Marijuana has a tetrahydrocannabinol (THC) content of more than 0.3% per plant dry weight, while hemp has a THC content of less than 0.3% per plant dry weight, which is a quantity within legal limits. Therefore, hemp is suitable for both medical and industrial applications in the health sector. However, distinguishing between marijuana and hemp, particularly during the plant's growth stages, is challenging due to their genetic and morphological similarities. Using Inter-Simple Sequence Repeats (ISSR) molecular marker techniques can quickly and accurately find the genetic diversity and tell the difference between hemp and marijuana plants. This research aims to analyze the differences between marijuana and hemp strains, specifically 12 strains, using a set of primers targeting the ISSR region. Utilizing polymerase chain reaction (PCR) techniques and analyzing the generated DNA patterns on Polyacrylamide gel, it was found that the DNA patterns generated from the 11 ISSR primers yielded a total of 230 bands, comprising 8.26% monomorphic bands (19 bands) and 91.74% polymorphic bands (211 bands). Genetic relationship analysis using the Unweighted Pair-group Method Arithmetic average (UPGMA) method revealed that ISSR markers could distinctly separate between Thai marijuana-hemp cultivars (Foithong, Hangkrarok, RPF1, and RPF2). Additionally, ISSR markers were able to differentiate between Thai marijuana and hemp strains. Hence, these ISSR markers serve as fundamental data for verifying marijuana and hemp plant groups in various hybrid strains and as foundational data for future plant breeding improvements.

Keywords: *Cannabis*, marijuana, hemp, ISSR marker.



Introductions

Cannabis plants, classified under the Cannabaceae family, hold significant medicinal and industrial value. These plants are generally categorized into two main types: medicinal cannabis, containing cannabidiol (CBD) levels below 0.3% and Δ^9 -tetrahydrocannabinol (THC) levels above 0.3%, and fiber hemp, with THC levels below 0.3% (Hesami *et al.*, 2020). Medicinal cannabis is utilized for various medical purposes, including pain relief and sleep aids, while hemp serves a multitude of commercial applications, such as textiles, paper, pharmaceuticals, food, and animal feed (Rehman *et al.*, 2021).

Current cannabis strains are available with high THC levels for medicinal use and high CBD levels for industrial hemp, extracted from the flower buds (Zhang *et al.*, 2018). Differentiating between these strains can be challenging but is achievable through methods such as physiological characteristics, chemical compounds, and DNA molecular markers. Each method has its strengths and limitations: morphological isolation allows for easy visual differentiation; cannabinoid profiling is useful when the plant is not visible; and DNA molecular markers can identify the desired cannabis strain at the seedling stage.

Genetic variations at the DNA level are detectable using molecular markers like restriction fragment length polymorphism (RFLP), random amplified polymorphic DNA (RAPD), amplified fragment length polymorphism (AFLP), and inter-simple sequence repeat (ISSR) (Liu *et al.*, 2008). ISSRs, regions in the genome surrounded by microsatellite sequences, can serve as a dominant multi-locus marker system for studying genetic variation (Ng & Tan, 2015).

Poolsawat *et al.* utilized the ISSR and ISSR-RGA techniques to detect powdery mildew resistance genes by analyzing a cross between a susceptible strain (CN72) and a resistant strain (V4718) of mung beans, identifying 5 ISSR and 3 ISSR-RGA markers associated with resistance, which are useful for breeding PM-resistant mung bean cultivars (Poolsawat *et al.*, 2017). In another study, Rout and Aparajita used ISSR markers to study 23 *Ficus* accessions, producing unique fingerprint profiles for each accession, detecting 30 species-specific bands, and evaluating genetic relationships using the UPGMA dendrogram (Rout & Aparajita, 2009). Additionally, Lata *et al.* evaluated the genetic stability of *Cannabis sativa* using ISSR markers, confirming genetic stability between clones and parent plants (Lata *et al.*, 2009).

This research aims to use DNA markers to identify THC and CBD dominance in cannabis strains early in the seedling stage, thus accelerating the selection process during breeding. Among the available DNA marker methods, this study focuses on ISSRs due to their suitability for non-plant models like cannabis, low cost, ease of use, and applicability without prior DNA sequence data (Barth *et al.*, 2002). The goal is to differentiate between Thai and foreign cannabis strains, enhancing agricultural applications in Thailand.

Materials and Methods

Plant material

The DNA was obtained from the leaves of 12 different cannabis strains collected from "SUT Cannabis Farm" located in Suranaree University of Technology, Suranaree, Mueang, Nakhon Ratchasima, 30000 (Table 1). The cannabis DNA were extracted using the cetyltrimethylammonium bromide (CTAB) method, and the DNA from each sample was diluted to 50 ng/μL for PCR amplification.

Table 1 The cannabis information

Name of cannabis groups			
Thai cultivars	foreign cultivars	Thai cultivars	foreign cultivars
Foithong	Blue Venom	RPF1	Baox
Hangkalok	Golden Tiger	RPF2	Cannafuel
	Orange Valley		Charlotte's Angle
	West Slope		Charlotte's Web

ISSR primers selection

A total of 38 ISSR primers referenced from research of mung bean because the absence of a cannabis-specific ISSR marker. The 11 ISSR primers with clear and reproducible bands were selected to amplify all cannabis strains (Table 2).

Table 2 ISSR primers selection

Primer cods	Sequences	Annealing temperature (°C)
ISSR 810	(GA)8T	55
ISSR 811	(GA)8C	55
ISSR 825	(AC)8T	53
ISSR 834	(GA)8YT	53
ISSR 841	(GA)8YC	48
ISSR 844	(CT)8RC	53
ISSR 880	(GGAGA)3	48
ISSR 888	BDB (CA)7	55
ISSR 891	HVH (TG)7	55
ISSR 895	(AG)2TTGGTAG (CT)2TGATC	48
ISSR 899	CATG(GT)2TGGT CATTGTTCCA	48

B = C, G, T ; N = A, G, C ; Y = pyrimidines (C, T) ; D = A, G, T ; R = purines (A, G) ; H = A, C, T ; V = A, C, G (Poolsawat *et al.*, 2017)

ISSR amplification and detection of DNA bands.

Approximately 50 ng of template DNA was added to a 10- μ L PCR mix containing 1x DreamTaq PCR Master Mix, 0.2 mM dNTPs, 1 mM primers, and 1.25 units of DreamTaq DNA Polymerase. The amplification program were consist of an initial denaturation at 94°C for 4 minutes, followed by 35 cycles of denaturation at 94°C for 20 seconds, annealing at a temperature dependent on the primer for 50 seconds, and extension at 69°C for 1 minute. The entire reaction was carried out in the BioRAD S1000 Thermal cycler. The PCR product quality was checked in a 1.0% agarose gel, using 3 μ L of the PCR reaction and the remaining reaction was then subjected to electrophoresis on a 3% polyacrylamide gel, consisting of 40% acrylamide/bis-acrylamide, 19:1 (5% crosslinker) solution) 3.6 mL, 10xTAE 2.4 mL, TEMED 16 μ L, 10% APS (ammonium peroxydisulfate, Biosharp) 160 μ L, and ddH₂O to a total volume of 24 mL. Electrophoresis was carried out in 1xTAE buffer at 220 U for 30 min. Gels were stained with 0.2% silver nitrate following a chromogenic reaction with 2% Na₂CO₃ (including 0.2% formaldehyde). This method, adapted from (Ji *et al.*, 2007), was optimized for my work, and the DNA pattern was finally observed under the "Molecular Imager Gel Doc XR System".

DNA pattern scoring.

Eleven markers were used to analyze the relationship of cannabis strains. The allelic data were converted into a binary matrix using the scores 1 and 0 for the presence and absence of the allele, respectively. Diversity patterns were represented in the form of a dendrogram, which was generated by subjecting the genetic similarity matrix to Unweighted Pair-group Method Arithmetic average (UPGMA) cluster analysis using the software NTSYS-pc, Version 2.0. (Rohlf, 1988).

Results and Discussion

ISSR primers selection and amplification

Thirty-eight ISSR primers were screened to identify polymorphic DNA bands among 12 cannabis strains, 19 ISSR primers successfully generated DNA bands. However, only 11 ISSR primers produced clear, reproducible, and polymorphic DNA bands. Consequently, these 11 ISSR primers were selected for further cannabis strain screening. These primers exhibited wide variation between strains, with optimal annealing temperatures of 55°C, 53°C, and 48°C (Table 2.). In total, these 11 primers amplified 230 scoreable DNA bands, ranging from 18 bands to 22 bands per primer, with an average of 20.9 bands per primer, comprising 8.26% monomorphic bands (19 bands) and 91.74% polymorphic bands (211 bands).

Table 3 Information of 11 ISSR primers

Primers	Primer sequences	Total number of fragments	Number of Polymorphic	Percentage of Polymorphism
ISSR 810	GAGAGAGAGAGAGAT	150-3000	19	89.47
ISSR 811	GAGAGAGAGAGAGAC	150-3000	20	90.00
ISSR 825	ACACACACACACACT	250-3000	18	88.89
ISSR 834	GAGAGAGAGAGAGAYT	250-3000	18	88.89
ISSR 841	(GA)8YC	150-3000	22	95.45
ISSR 844	(CT)8RC	250-3000	18	88.89
ISSR 880	(GGAGA)3	250-3000	21	90.48
ISSR 888	BDB (CA)7	150-3000	21	95.24
ISSR 891	HVH (TG)7	350-3000	20	90.00
ISSR 895	GAGATTGGTAGCTCTTGATC	300-3000	17	88.24
ISSR 899	CATG(GT)2TGGT CATTGTTCCA	300-3000	17	94.12
Total			211	

The high polymorphism rate observed in this study was consistent with findings in other plant species where ISSR markers have been used to assess genetic diversity. Shahabzadeh *et al.* (2019) found significant genetic diversity in Tall festuca populations using ISSR markers, demonstrating their utility in distinguishing genetic variations within species (Shahabzadeh *et al.*, 2020).

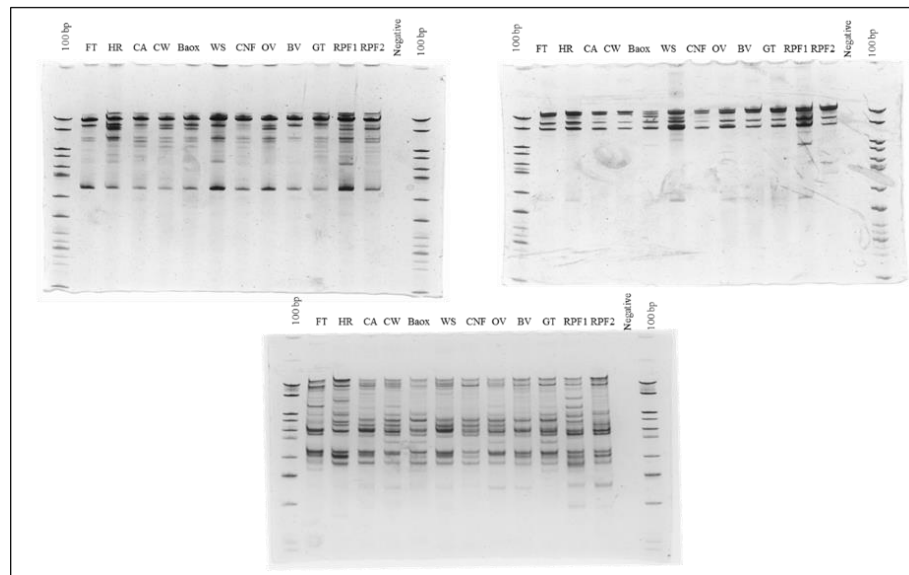


Figure 1 DNA pattern of 12 cannabis strains using ISSR markers observe in polyacrylamide gels

Genetic Diversity

The DNA pattern was observed in polyacrylamide gel and scored, then used UPGMA to generate relationship among 12 cannabis strains. The dendrogram showed coefficient of similarity length 0.62 to 0.81 and it revealed that the cannabis strains could be segregated into two main clusters: Cluster 1 comprised nine cannabis strains: FoiThong, Hangkarok, Charlotte’s Angel, Cannafuel, West Slop, Charlotte’s Web, Orange Valley, BaOx, and Golden Tiger, while Cluster 2 consisted of three cannabis strains: Blue Venom, RPF1 and RPF2.

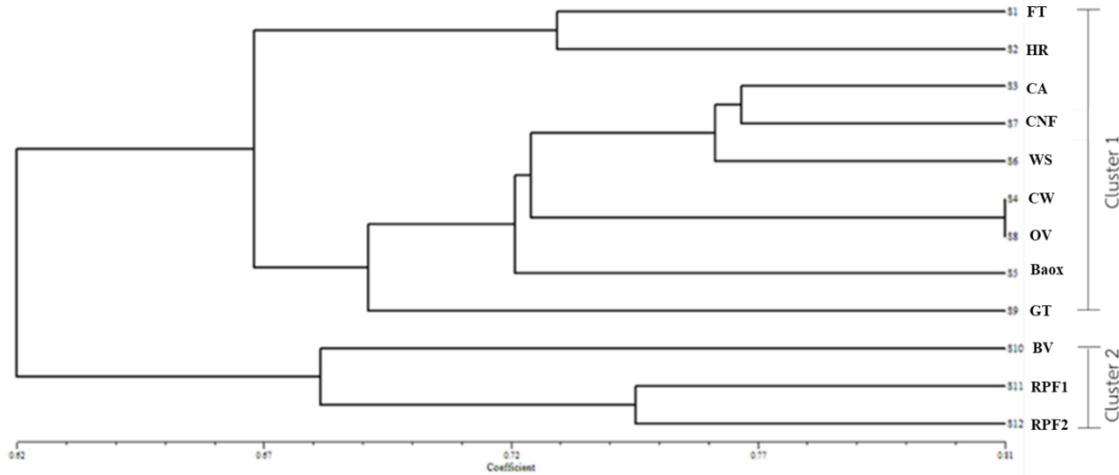


Figure 2 Dendrogram illustrating the genetic relationship analysis of 12 cannabis strains

Genetic relationship analysis using the UPGMA method revealed that ISSR markers could distinctly separate 12 cannabis strains. Additionally, ISSR markers were able to differentiate between Thai marijuana and hemp cultivars. Using the UPGMA method for genetic relationship analysis, this study successfully distinguished between Thai marijuana-hemp cultivars. This distinct separation aligns with the findings of Gao *et al.* (2014), who employed SSR markers to reveal significant genetic variation among cannabis samples, thus supporting the reliability of molecular markers in genetic differentiation (Gao *et al.*, 2014)

This study further demonstrated that ISSR markers could differentiate between Thai marijuana and hemp strains. This capability was crucial for plant verification and breeding programs. The genetic distinctions observed in this study provide foundational data for verifying cannabis plant groups and improving breeding strategies. These findings were corroborated by previous studies on various plant species, including cannabis, where molecular markers have been successfully used to identify and differentiate between cultivars and strains (Nurhasanah *et al.*, 2023)

Conclusions

The significant polymorphism rate revealed by ISSR markers in this study underscores their effectiveness in detecting genetic diversity among cannabis strains. This demonstrates the utility of ISSR markers in cannabis research, offering valuable data for verifying plant groups within hybrid strains and establishing a foundation for future advancements in plant breeding.



Acknowledgements

First of all, I would like to thank Suranaree University of Technology and the OROG Scholarship for the financial support that made this work possible.

I am deeply grateful to my advisor, Professor Dr. Neung Teaumroong, and co-advisors, Professor Kamolchanok Umnajkitikorn and Assoc. Prof. Dr. Panlada Tittabutr, for their valuable advice and support throughout my research.

Sincerely, thank SUT Cannabis Farm, especially Professor Dr. Nantakorn Boonkerd, for providing all the cannabis strains used in this research.

Thank you to Professor Dr. Piyada Alisha Tantasawat for supporting the primers for my work and Mr. Wisarut Chuakhunthod for assisting with filtering and analysis techniques.

I appreciate the support and assistance from Dr. Kamonlak Teamitisong, Dr. Pongdet Phiromyou, Dr. Pongphan Songwattana, Dr. Jenjira Wongdee, Dr. Teerana Kritathorn, and Asst. Prof. Pakpoom Boonchuen in using equipment and solving laboratory problems.

Finally, I am forever indebted to my family for their unwavering support and financial assistance, without which this work would not have been possible.

References

- Barth, S., Melchinger, A. E. and Lübberstedt, T. 2002. Genetic diversity in *Arabidopsis thaliana* L. Heynh. Investigated by cleaved amplified polymorphic sequence (CAPS) and inter-simple sequence repeat (ISSR) markers. *Molecular Ecology*, 11(3): 495–505. <https://doi.org/10.1046/j.0962-1083.2002.01466.x>
- Gao, C., Xin, P., Cheng, C., Tang, Q., Chen, P., Wang, C., Zang, G. and Zhao, L. 2014. Diversity Analysis in *Cannabis sativa* Based on Large-Scale Development of Expressed Sequence Tag-Derived Simple Sequence Repeat Markers. *PLoS ONE*, 9(10), e110638. <https://doi.org/10.1371/journal.pone.0110638>
- Hesami, M., Pepe, M., Alizadeh, M. and Rakei, A. 2020. *Recent advances in cannabis biotechnology | Request PDF*. https://www.researchgate.net/publication/344862959_Recent_advances_in_cannabis_biotechnology
- Ji, Y., Qu, C. and Cao, B. 2007. An optimal method of DNA silver staining in polyacrylamide gels. *ELECTROPHORESIS*, 28(8), 1173–1175. <https://doi.org/10.1002/elps.200600557>
- Kojoma, M., Iida, O., Makino, Y., Sekita, S. and Satake, M. 2002. *DNA fingerprinting of Cannabis sativa using inter-simple sequence repeat (ISSR) amplification—PubMed*. <https://pubmed.ncbi.nlm.nih.gov/11842329/>
- Lata, H., Chandra, S., Techen, N., Khan, I. A. and ElSohly, M. A. 2009. Assessment of the Genetic Stability of Micropropagated Plants of *Cannabis sativa* by ISSR Markers. *Planta Medica*, 76: 97–100. <https://doi.org/10.1055/s-0029-1185945>



- Liu, L.-W., Zhao, L.-P., Gong, Y.-Q., Wang, M.-X., Chen, L.-M., Yang, J.-L., Wang, Y., Yu, F.-M. and Wang, L.-Z. 2008. DNA fingerprinting and genetic diversity analysis of late-bolting radish cultivars with RAPD, ISSR and SRAP markers. *Scientia Horticulturae*, 116(3), 240–247. <https://doi.org/10.1016/j.scienta.2007.12.011>
- Ng, W. L. and Tan, S. G. 2015. *Inter-Simple Sequence Repeat (ISSR) Markers: Are We Doing It Right?*
- Nurhasanah, Hindersah, R., Suganda, T., Concibido, V., Sundari and Karuniawan, A. 2023. The First Report on the Application of ISSR Markers in Genetic Variance Detection among Butterfly Pea (*Clitoria ternatea* L.) Accession in North Maluku Province, Indonesia. *Horticulturae*, 9(9), Article 9. <https://doi.org/10.3390/horticulturae9091059>
- Poolsawat, O., Kativat, C., Arsakit, K. and Tantasawat, P. 2017. *Identification of quantitative trait loci associated with powdery mildew resistance in mungbean using ISSR and ISSR-RGA markers | Request PDF.* https://www.researchgate.net/publication/321122583_Identification_of_quantitative_trait_loci_associated_with_powdery_mildew_resistance_in_mungbean_using_ISSR_and_ISSR-RGA_markers
- Rehman, M., Fahad, S., Du, G., Cheng, X., Yang, Y., KaileiTang, K., Liu, L., Liu, F.-H. and Deng, G. 2021. *Evaluation of hemp (Cannabis sativa L.) as an industrial crop: A review —Pub Med.* <https://pubmed.ncbi.nlm.nih.gov/34476693/>
- Rohlf, F. 1988. NTSYS-pc—Numerical Taxonomy and Multivariate Analysis System. *Applied Biostatistics Inc. New York, 2.1.*
- Rout, G. and Aparajita, S. 2009. Genetic relationships among 23 *Ficus* accessions using inter-simple sequence repeat markers. *Journal of Crop Science and Biotechnology*, 12, 91–96. <https://doi.org/10.1007/s12892-009-0095-7>
- Shahabzadeh, Z., Mohammadi, M., Darvishzadeh, R. and Jaffari, M. 2020. *Genetic structure and diversity analysis of tall fescue populations by EST-SSR and ISSR markers—PubMed.* <https://pubmed.ncbi.nlm.nih.gov/31707600/>
- Zhang, H.-L., Jin, J., Moore, M., Yi, T. and Li, D.-Z. 2018. Plastome characteristics of Cannabaceae. *Plant Diversity*, 40. <https://doi.org/10.1016/j.pld.2018.04.003>



Evaluation of Dust Quality from Cement Products for Agricultural Applications

Kantakapun, K.¹

¹ Department of Chemical Engineering, Faculty of Engineering, Prince of Songkla University, Songkhla 90112

* Corresponding author: kjutharat@eng.psu.ac.th

Abstract

The ready-mixed concrete manufacturing industry from 2021 to 2023 is expected to grow at a rate of 4.0-5.0% per year, with an annual volume of 16 million cubic meters. However, the production process generates a significant amount of cement dust, which primarily contains calcium (Ca) or a combination of Ca and magnesium (Mg). This research aims to understand the chemical and physical properties of the samples and analyze their applicability according to the standards for agricultural lime materials. The quality of the samples was tested for chemical and physical properties, including mineral composition using X-Ray Diffractometer (XRD) and X-ray fluorescence Spectrometer (XRF), pH level, moisture content, and Calcium Carbonate Equivalent (CCE). Physical properties were assessed by particle size distribution for agricultural lime. The samples were collected from stone mills. The study results showed that the CCE value was 95%, Calcium Oxide (CaO) content was 49.17%, pH was 9.0, particle size passing through 8 mesh and 80 mesh sieves was 100%, and moisture content was 0.4%. These properties indicated that the lime materials derived from the ready-mixed concrete production process meet the standards for agricultural applications, such as soil pH adjustment and providing essential nutrients for plant growth. Additionally, utilizing these materials can help reduce dust emissions from stone mills.

Keywords: lime, agriculture, ready-mixed concrete, dust

Introduction

The production of ready-mixed concrete is a cornerstone of modern construction, underpinning infrastructure development across the globe. This industry, valued for its efficiency and product durability, produced approximately 16 million cubic meters annually over the past few years, witnessing a growth rate of 4.0–5.0% per annum from 2021 to 2023 (Grand View Research, 2023; Allied Market Research, 2023). Despite its significant contributions to construction, the industry is also a source of considerable environmental concern, primarily due to the emission of cement dust during manufacturing processes. This dust, predominantly composed of Ca or a combination of Ca and Mg, poses risks to environmental health and occupational safety (Adeyanju & Okeke, 2019). However, these by-products also present potential opportunities for beneficial reuse, particularly in agriculture.

Agricultural lime, a critical amendment in agriculture, is used to increase soil pH levels, improve soil structure, and augment nutrients availability in acid soil to plants. Traditionally sourced from natural limestone, the feasibility of substituting this material with by-products from industrial processes such as cement dust could not only provide a sustainable disposal pathway but also reduce the environmental



footprint of both industries (Akash Nevel, et al. 2024). This research aims to rigorously evaluate the chemical and physical properties of cement dust generated from the ready-mixed concrete industry, assessing its suitability as a substitute for traditional agricultural lime.

This paper presents an extensive analysis of the mineral composition, pH levels, moisture content, and CCE of the cement dust. Employing advanced analytical techniques such as XRD and XRF alongside standard physical property assessments, this study provides a comprehensive evaluation aligned with the standards set by the Land Development Department (LDD) (LDD, 2010). The implications of using this by-product in agricultural settings are discussed, with an emphasis on environmental sustainability and economic viability. Through this investigation, the study aims to bridge the gap between industrial by-product management and agricultural enhancement, contributing to the circular economy model in industrial practices.

Materials and Methods

1. Sample Collection

Cement dust samples were systematically collected from stone mills involved in the production of ready-mixed concrete.

2. Chemical Analysis

2.1 Calcium Carbonate Equivalence (CCE)

The CCE was determined to evaluate the purity of the liming material, which is critical in assessing its effectiveness in agriculture. A CCE of 100% indicates equivalence to pure calcium carbonate, which is ideal for soil amendment.

2.2 Mineral Composition Analysis

1) X-Ray Diffractometer (XRD): This technique was utilized to determine the atomic and molecular structure of the samples. The process involves irradiating the material with X-rays and measuring the scattering angles and intensities of the reflected beams. The data obtained helps in identifying the crystalline structure and detecting any structural deviations or defects.

2) X-ray Fluorescence Spectrometer (XRF): To ascertain the elemental composition of the samples, XRF analysis was employed. This method uses the fluorescence produced by a material when bombarded with X-rays to identify and quantify the elements present. Each element emits a unique spectral fingerprint, making XRF a powerful tool for qualitative and quantitative assessments.

2.3 pH Level Determination

The pH of the cement dust was measured by adapting the method typically used for soil pH testing. Approximately 10 g of dust was mixed with 50ml of distilled water to create a 1:5 dilution (w/v). The mixture was agitated for 2-3 minutes and allowed to settle for 2 minutes before the pH of the supernatant was measured using a digital pH meter.

3. Physical Analysis

3.1 Particle Size Distribution

Physical properties, particularly particle size, were assessed using sieving methods. Samples were passed through 8 mesh and 80 mesh sieves to determine the distribution of particle sizes. This method helps in evaluating the suitability of the material for agricultural use by ensuring the particles are within the desired size range for effective soil modification.

3.2 Moisture Content Assessment

Moisture content was quantified by the mass of water relative to the solid mass of the sample, expressed as a percentage. The standard procedure involved drying a known weight of the sample at $110 \pm 5^\circ\text{C}$ and calculating the percentage of moisture content (M_c) using the formula:

$$M_c(\%) = \left(\frac{W - d}{W} \right) \times 100 \tag{1}$$

where W is the initial wet weight
 d is the dry weight after heating

Results

The analysis of cement dust samples collected from stone mills aimed to evaluate their suitability as a substitute for traditional agricultural lime. The result from the study shows in Table 1.

Table 1 Analysis of properties according to product standards for agricultural lime

Properties	Standards criteria	Results
Calcium Carbonate Equivalent (CCE, %)	> 85	95
Calcium Oxide (CaO, %)	> 40	49.17
pH Level	> 8.0	9.0
Particle Size Passing Through 8 Mesh (%)	> 85	100
Particle Size Passing Through 80 Mesh (%)	> 50	100

Note: The standards criteria by the LDD for agricultural lime (LDD, 2010).

Table 1 demonstrates that the cement dust exceeds standard values in all listed categories, making it an exceptional candidate for agricultural lime applications. The results from the study are as follows:

1. Calcium Carbonate Equivalence (CCE)

The CCE is a key parameter used to assess the quality and effectiveness of liming materials. A CCE of 95% indicates that the cement dust has nearly the same neutralizing power as pure calcium carbonate, which is considered the standard for agricultural lime due to its high efficacy in soil pH adjustment. This high percentage means that the dust is predominantly composed of materials that react similarly to calcium carbonate when interacting with acidic soils.

The significance of a 95% CCE is substantial in the context of agriculture. It suggests that the cement dust can effectively raise soil pH, thus helping to ameliorate acidic soils and make them more suitable for

crop cultivation. By increasing the pH, the availability of essential nutrients to plants is improved, and toxic elements in the soil can become less available, thereby promoting healthier crop growth.

2. Calcium Oxide (CaO)

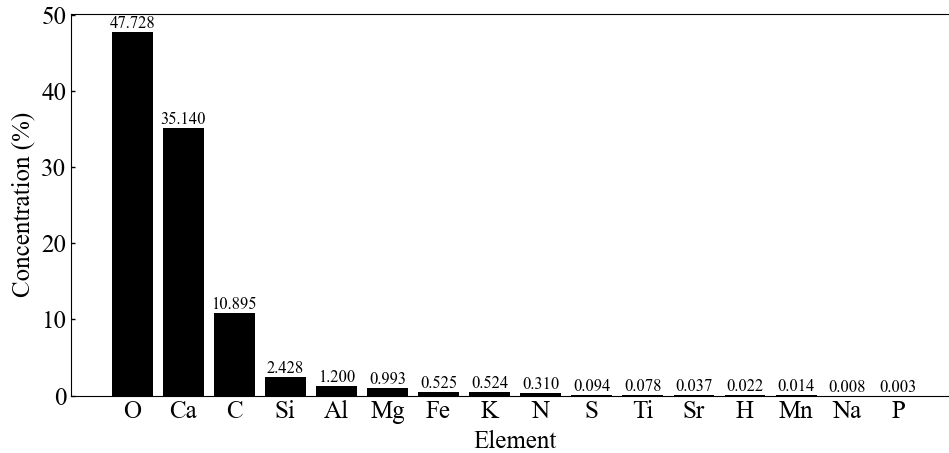


Figure 1 The elemental concentration by X-ray Fluorescence (XRF)

The Figure 1 clearly shows the concentrations of various elements in the sample:

1) Primary Elements

The graph prominently features Oxygen (O) at 47.728%, Calcium (Ca) at 35.14% and Carbon (C) at 10.895%, making them the most significant constituents of the sample. These elements are crucial for confirming the presence of $CaCO_3$, which is consistent with the high CCE of 95%.

2) Minor Elements

Silicon (Si), Aluminum (Al), Magnesium (Mg), Iron (Fe), and Potassium (K) appear in smaller percentages but are significant for the overall mineral matrix of the cement dust. These elements contribute to the physical and chemical properties of the dust.

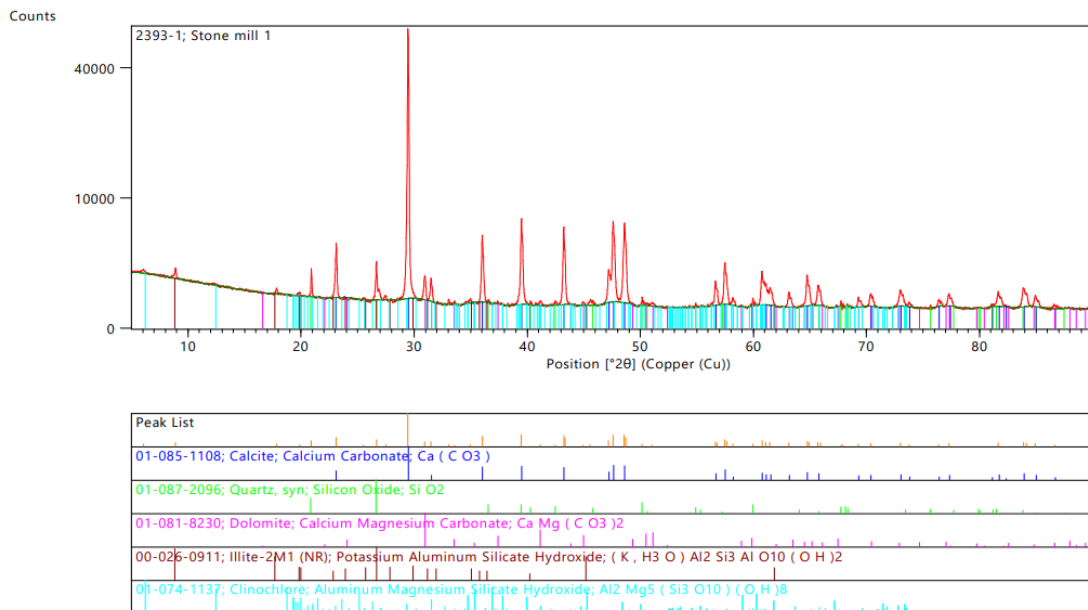


Figure 2 The X-Ray Diffraction (XRD) pattern from a sample of cement dust from stone mill



The Figure 2 shows the most significant peak occurs around the 2Theta value of approximately 29.4°, which is indicative of Calcite (CaCO_3). Calcite is the primary phase and is responsible for the cement dust's capacity to neutralize acid in soil, correlating to its high CCE.

The quantitative and qualitative analyses of the cement dust using XRD and XRF techniques revealed significant insights into its chemical and mineralogical composition, particularly concerning the CaO content. XRD analysis successfully identified the crystalline forms of CaO present in the sample, confirming the mineral's existence alongside other compounds such as calcium carbonate. These results are crucial as they indicate that the CaO is likely available in a reactive form suitable for soil amendment purposes.

Simultaneously, XRF analysis provided a precise quantification of the elemental calcium present in the dust, measured at 35.14%. Using the stoichiometric conversion of elemental calcium to CaO, based on their respective molar masses, the CaO content was calculated to be approximately 49.17% as follows:

$$\text{CaO}(\%) = \left(\frac{\text{Molar mass of CaO}}{\text{Molar mass of Ca}} \right) \times \text{Ca} (\% \text{ from XRF}) \quad (2)$$

Where Molar mass of CaO = 56.077 g/mol

Molar mass of Ca = 40.078 g/mol

Ca (from XRF) = 35.14%

Figure 2 not only underscores the richness of the dust in terms of lime content but also corroborates its potential efficacy as a soil amendment agent. The high percentage of CaO is instrumental in enhancing the material's property to neutralize soil acidity, thereby improving soil health and agricultural productivity.

3. pH Level

The study results indicating a pH of 9.0 for the cement dust are notably above the standard threshold of greater than 8.0. This indicates a higher alkalinity than the minimum required for effective agricultural lime applications. In agricultural practices, lime is frequently utilized to increase soil pH to a more neutral level, which is crucial for optimal plant growth and nutrient uptake (Miller, 2019). The pH level of 9.0 not only meets but exceeds the standard, suggesting enhanced potential for soil amendment.

4. Particle Size Distribution

The results of our study demonstrate that the particle size distribution of cement dust is exceptionally fine, with 100% of the particles successfully passing through both 8 mesh and 80 mesh sieves. This level of fineness significantly surpasses the established industry standards, which mandate that only more than 85% of particles should pass through an 8 mesh sieve and more than 50% through an 80 mesh sieve. The comprehensive passage of cement dust particles through these sieves confirms its superior quality and uniformity compared to typical agricultural lime products. The fine particle size is crucial, as it ensures enhanced reactivity and more homogeneous soil amendment capabilities, promoting more consistent pH modification and nutrient distribution within treated soils.

5. Moisture Content (%)

Table 2 provided in the study details the moisture content measurements for cement dust samples. Three samples were weighed, with weights recorded as 5.023, 5.053 and 5.041 g, respectively. The respective



moisture contents were 0.39%, 0.43%, and 0.37%. These individual measurements were used to calculate an average moisture content of 0.40%, with a standard deviation (SD) of 0.03% and a percent relative standard deviation (RSD) of 7.70%. The %RSD indicates the degree of variance in relation to the average, providing insight into the consistency of the moisture content across different samples. Therefore, the moisture content of the cement dust was found to be $0.4\% \pm 0.03\%$, which is significantly lower than the standard. This indicates exceptional quality control in the production or processing of the cement dust, ensuring that it remains dry and free from excess moisture that could complicate its use in agricultural settings.

Table 2 The moisture content analyses for cement dust samples

Name	weight sample (g)	Moisture (%)	Average	SD	%RSD
Cement dust	5.023	0.39	0.40	0.03	7.70
	5.053	0.43			
	5.041	0.37			

Discussion

The utilization of industrial by-products in agriculture has been explored in several studies, highlighting both potential benefits and concerns. The CCE of 95% indicates a highly effective neutralizing power, surpassing the standard requirement of 85%. This high CCE means the soil amendment can more effectively counteract soil acidity, improving soil health and fertility. Research shows that materials with higher CCE values provide better pH adjustments, which is crucial for optimal plant growth (Olego et al., 2021). With a CaO content of 49.17%, this soil amendment exceeds the typical standard of 40%. Higher CaO levels enhance the soil's structure by increasing its calcium content, which can help in flocculating clay particles, thereby improving soil aeration and water infiltration. Studies confirm that elevated CaO levels in soil amendments contribute to better soil physical properties and nutrient availability. A pH of 9.0 significantly exceeds the standard threshold of 8.0, indicating the amendment's strong alkalinity, which is beneficial for raising soil pH and reducing soil acidity, the toxicity of Fe and Al to plant growth grown in acid soils. This change in pH can create a more favorable environment for nutrients uptake by plants. The effectiveness of liming materials in adjusting soil pH is well-documented, and higher pH levels can improve microbial activity and nutrient availability (Yu et al., 2023). The fact that 100% of the particles pass through both 8 and 80 mesh sieves ensures a fine particle size, which is crucial for the rapid and uniform distribution in the soil. Finer particles increase the surface area exposed to soil acidity, enhancing the speed and uniformity of the pH adjustment. Research emphasizes the importance of particle fineness for the effectiveness of lime in neutralizing soil acidity (Mamo, et al., 2009). A moisture content of 0.4 is well below the maximum standard of 5%, ensuring that the soil amendment is stable and easy to handle. Low moisture content prevents clumping and ensures consistent application. Stability and ease of handling are critical for practical agricultural use, ensuring that the material can be spread evenly across fields without issues. Therefore, cement dust from stone mill can be used for soil amendment in agricultural applications. For example, using cement dust from stone mills as a soil amendment offers substantial benefits for agricultural applications, particularly in

improving acid soils. Its high CCE, elevated CaO content, strong alkalinity, fine particle size, and low moisture content collectively contribute to enhancing soil health and fertility, leading to better crop growth and productivity (Guyer, 2017). This research underscores the potential of industrial by-products in sustainable agriculture, providing a cost-effective solution for soil improvement and environmental management.

Conclusions

The comprehensive evaluation of cement dust for potential agricultural applications revealed that it significantly exceeds the established quality standards for agricultural lime, according to criteria set by the Land Development Department. With a CCE of 95% and a CaO content of 49.17%, the dust demonstrates exceptional neutralizing power, comparable to pure calcium carbonate. This ensures its efficacy in increasing soil pH well above the standard minimum of 8.0, as evidenced by the measured pH of 9.0. Moreover, the particle size analysis showed that 100% of the dust passed through both 8 mesh and 80 mesh sieves, surpassing the standard requirements of >85% and >50% respectively, which guarantees a fine particle distribution for even soil amendment. The remarkably low moisture content of 0.4% also highlights the dust's suitability for storage and ease of application, preventing caking and ensuring stability. Collectively, these results not only validate the use of cement dust as a high-quality, effective alternative to traditional agricultural lime but also underscore its role in promoting sustainable agricultural practices through the repurposing of industrial by-products. This study advocates for the expanded use of cement dust in agriculture, aiming to enhance soil health, increase crop productivity, and contribute to environmental sustainability.

References

- Adeyanju, E., Okeke, C.A. 2019. Exposure effect to cement dust pollution: a mini review. *SN Appl. Sci.* 1.
- Akash Nevel, R., Dinesh Kumar, R., Surendar, M. 2024. Review on Partially Replacement of Cement with Industrial Waste in Manufacturing of Concrete and Bricks. In *Sustainable Innovations in Construction Management. ICC IDEA 2023. Lecture Notes in Civil Engineering* (eds. Gencel, O., Balasubramanian, M., Palanisamy, T.) Vol 388. Springer: Singapore.
- Allied Market Research. 2024. Ready-Mix Concrete Market Size, Trends, Forecast 2030. Available from: <https://www.alliedmarketresearch.com/ready-mix-concrete-market-A06028> [accessed on 5 June 2024].
- Grand View Research. 2024. Ready-mix Concrete Market Size and Share Report, 2030. Available from: <https://www.grandviewresearch.com/industry-analysis/ready-mix-concrete-market> [accessed on 5 June 2024].
- Guyer, J. P. 2017. *An Introduction to Soil Stabilization with Portland Cement*. NJ: Continuing Education and Development, Inc.
- LDD. 2010. The standards criteria for agricultural lime. Available from: <http://ord101.ldd.go.th/webmordin/องค์ความรู้/การใช้วัสดุปูนเพื่อการเกษตร%20ในการปรับปรุงดิน.pdf> [accessed on 5 June 2024].
- Mamo, M., Wortmann, C. S., Shapiro, C. A. 2009. Lime Use for Soil Acidity Management. Available from: <https://extensionpubs.unl.edu/publication/g1504/html/view> [accessed on 5 June 2024].



- Miller, L. 2019. Lime and liming – managing soil health. Available from: <https://grdc.com.au/resources-and-publications/grdc-update-papers/tab-content/grdc-update-papers/2019/02/lime-and-liming-managing-soil-health> [accessed on 5 June 2024].
- Olego, M.Á., Quiroga, M.J., Mendaña-Cuervo, C., Cara-Jiménez, J., López, R., Garzón-Jimeno, E. 2021. Long-Term Effects of Calcium-Based Liming Materials on Soil Fertility Sustainability and Rye Production as Soil Quality Indicators on a Typic Palexerult. *Processes* 9: 1181.
- Yu, X., Keitel, C. & Dijkstra, F.A. 2023. Ameliorating soil acidity with calcium carbonate and calcium hydroxide: effects on carbon, nitrogen, and phosphorus dynamics. *J Soil Sci Plant Nutr* 23: 5270–5278.



Production and Purification Recombinant Vago1 Protein for Antibody Generation

Aunkam, P.¹, Seabkongseng, T.¹, Limkul, S.¹, Suwantit, R.¹, Phiwthong, T.¹, and Boonchuen, P.^{1*}

¹ School of Biotechnology, Institute of Agricultural Technology, Suranaree University of Technology, Nakhon Ratchasima, Thailand 30000

*Corresponding author: pakpoom.b@sut.ac.th

Abstract

Vago1 belongs to the family of single domain von Willebrand factor type C (SVWC) proteins, which are crucial for the innate immunological defense systems of a variety of invertebrates. In the case of white shrimp Vago1, it has been reported that the system is infected with WSSV. Therefore, this research aims to produce and purify recombinant Vago1 protein for implementing in the context of biological functions. Firstly, the polymerase chain reaction (PCR) technique was employed to amplify Vago1 and the PCR product was ligated to expression plasmids using restriction enzyme digestion and DNA ligation techniques. The constructed plasmids were then transformed into expression bacteria to overexpress Vago1 protein. Protein purification was conducted by utilizing an affinity chromatography (Ni-NTA column). According to the outcomes of the experiment, the recombinant Vago1 protein can be successfully produced and purified, which could be used in further research topics to clarify our understanding of the role of Vago1 in the immune systems of invertebrates against pathogens.

Keywords: Vago1, Recombinant protein production, Protein purification

Introduction

Single domain von Willebrand factor type C (SVWC) proteins represent a diverse family of proteins characterized by a VWC domain. These proteins are predominantly found in invertebrates such as arthropods and mollusks, where they play crucial roles in various biological processes, including immune responses. Among these SVWC proteins, Vago1 has emerged as a significant player in the innate immune system of crustaceans, particularly in the Pacific white shrimp (*Penaeus vannamei*). Initially identified in *Drosophila melanogaster*, Vago1 shares functional similarities with mammalian interferons, acting through conserved signaling pathways like the JAK/STAT pathway to combat viral infections (Chen et al., 2014); (Liu et al., 2014).

In *Penaeus vannamei*, Vago1 serves as a critical component of the shrimp's defense against viral pathogens, notably the white spot syndrome virus (WSSV). Studies have demonstrated that Vago1 expression is regulated by interferon regulatory factors (IRFs), which modulate its levels in response to viral challenges. This regulatory mechanism highlights Vago1's pivotal role in coordinating the shrimp's antiviral responses, like immune responses observed in vertebrates (Li & Xiang, 2013); (He et al., 2019)

The implications of Vago1 extend beyond fundamental immunology to practical applications in shrimp farming. Given the economic importance of *Penaeus vannamei* aquaculture and the persistent challenges posed by diseases like WSSV, understanding Vago1's immune functions opens avenues for



enhancing disease resistance in farmed shrimp. Strategies aimed at manipulating Vago1 expression through dietary supplements or genetic approaches hold promise for improving shrimp health and reducing mortality rates, thereby supporting sustainable aquaculture practices (Shi et al., 2021); (Ma et al., 2008)

This study aims to produce and purify recombinant Vago1 protein for antibody generation, focusing on its application in shrimp farming. The Vago1 gene was amplified using PCR, cloned into expression plasmids, and then transformed into bacterial hosts for protein expression. Purification was conducted using affinity chromatography with a Ni-NTA column, ensuring the isolation of high-quality Vago1 protein. This purified protein was then used to generate antibodies, which hold promise for enhancing shrimp immune responses against viral pathogens like white spot syndrome virus (WSSV). These findings contribute to developing biotechnological tools that could potentially improve disease management practices and sustainability in shrimp aquaculture.

Materials and Methods

Cloning and Amplification of LvVago1 for Expression

For the construction of expression vectors harboring LvVago1, specific primer sets were designed for PCR amplification. The forward primer (5'-CATCCATGGGCAGTTCTTGCTGATTGCTTGCTT-3') included an NcoI restriction site at its 5' terminus to facilitate directional cloning, while the reverse primer (5'-GATGGATCCTTAATGATGATGATGATGATGATGATGATGAGCAGTTCCTGGTGCTGCTGTGG-3') incorporated a BamHI restriction site and a 6× His-tag at its 3' end for subsequent affinity purification of the recombinant protein. PCR amplification was conducted under optimal thermal cycling conditions: an initial denaturation step at 95°C, followed by 35 cycles of denaturation at 95°C for 30 seconds, annealing at 60°C for 30 seconds, and extension at 72°C for 30 seconds, with a final extension at 72°C for 10 minutes. Purification of the PCR products was carried out using the FavorPrep Gel/PCR Purification Mini Kit (Favorgen) to ensure the removal of contaminants and obtain pure DNA fragments. The purified PCR products were then digested with NcoI and BamHI restriction enzymes, ligated into the pET-22b vector, and subsequently transformed into competent cells for further expression analysis.

Expression of pET-22b/LvVago1 proteins in *Escherichia coli* strains

The pET-22b/LvVago1 expression vectors were transformed into *Escherichia coli* strains BL21 (DE3), BL21(DE3)-CodonPlus, and Rosetta (DE3) for protein expression. Cultures were cultivated until reaching an optical density at 600 nm (OD₆₀₀) of approximately 0.4–0.6. Subsequently, isopropyl β-D-1-thiogalactopyranoside (IPTG) was added to a final concentration of 1 mM to induce protein expression, which continued for 4 hours at 37°C with agitation at 250 rpm. Following induction, cellular lysates were subjected to centrifugation at 10,000 g for 15 minutes at 4°C. The resulting pellets were collected and stored at -80°C.

Purification and quantification of recombinant LvVago1 proteins

The Cells were harvested and resuspended in a binding buffer (6 M urea in 1xPBS pH 7.4 and 1% SDS in 1xPBS pH 7.4). Sonication was then performed, and inclusion bodies were collected and solubilized in a binding buffer supplemented with 6 M urea and 1% SDS. The mixture, containing 1% SDS in 1x PBS (pH 7.4),



was incubated on ice for 30 minutes before centrifugation to precipitate the SDS. The recombinant LvVago1 proteins were purified by the Ni-NTA agarose bead (GoldBio) column. Elution was performed using a buffer of 6 M urea and 1% SDS in 1x PBS (pH 7.4) with varying imidazole concentrations. Fractions containing the recombinant proteins were pooled and dialyzed. Protein concentration was determined using the Bradford assay (Bradford, 1976).

Confirmation of purified recombinant LvVago1 protein by western blot analysis

E. coli BL21-CodonPlus (DE3) strains harboring LvVago1 and recombinant LvVago1 protein were subjected to electrophoresis on a 12% SDS-PAGE gel. The resolved proteins were then transferred onto a nitrocellulose membrane using a semi-dry blotting technique (Amersham, Biosciences). The membrane was subsequently blocked with a 2% skim milk solution at room temperature for 1 hour. Following blocking, the membrane underwent five washes in 1x PBS containing 0.1% Tween 20. It was then incubated with mouse anti-His-Tag monoclonal antibody (ABclonal), diluted at a ratio of 1:5,000 in 2% skim milk with 0.05% Tween 20. After antibody incubation, the membrane underwent an additional five washes in 1x PBS with 0.1% Tween 20 and was subsequently incubated for 1 hour at room temperature with HRP-conjugated goat anti-mouse IgG (ABclonal), diluted at a ratio of 1:5,000 in 1x PBS containing 2% skim milk and 0.1% Tween 20. The membrane was then washed three times in 1x PBS with 0.1% Tween 20 for 5 minutes per wash. Chemiluminescent signals were detected using clarity Western ECL Substrate (Bio-Rad).

Results

Amplification and Cloning of LvVago1 Gene into pET22b Vector

The process of constructing the pET22b-LvVago1 plasmid begins with the PCR amplification of the LvVago1 gene, resulting in a specific PCR product (Figure 1A). This product is then ligated into the pET22b vector to create the recombinant pET22b-LvVago1 plasmid (Figure 1B). Following transformation into bacterial cells, the plasmid is extracted and purified. Verification of successful cloning is conducted by performing PCR colony screening on 10 selected colonies (Figure 1C). Additionally, the recombinant plasmid undergoes double digestion with NcoI and BamHI restriction enzymes, and the resulting digestion products are analyzed by electrophoresis on a 1% agarose gel to confirm the presence and accurate insertion of the LvVago1 gene (Figure 1D). It was found that successfully cloned the pET22b-LvVago1 plasmid, especially with a specific site size of 543 bp.

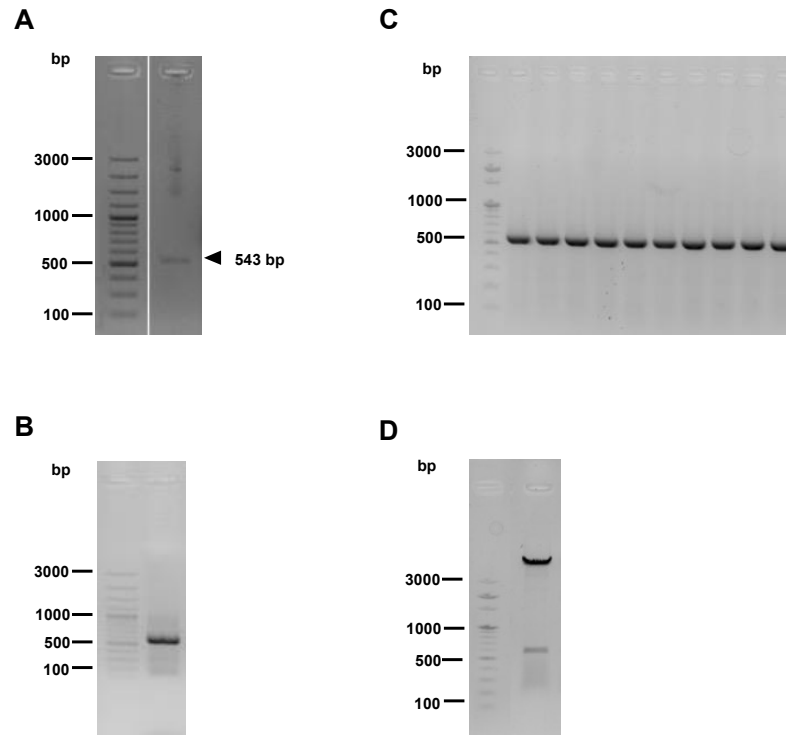


Figure 1 Amplification of LvVago1 gene and construction of pET22b-LvVago1 plasmid. (A) PCR product of LvVago1 gene, (B) pET22b- LvVago1 plasmid extraction result, (C): Select 10 colonies for PCR colony testing, (D): double digestion of recombinant pET22b-LvVago1 by NcoI and BamHI. Products were electrophoresed on 1% agarose gel.

Escherichia coli strains BL21 (DE3), BL21(DE3)-CodonPlus, and Rosetta (DE3) transformed with sequence-verified LvVago1 produced a 19 kDa protein after induction with IPTG

Following successful cloning of the pET22b-LvVago1 plasmid, which confirmed a 543 bp sequence (Figure 1), *Escherichia coli* strains BL21(DE3)-CodonPlus, BL21(DE3), and Rosetta (DE3) were transformed for protein expression studies. Induction with IPTG revealed robust production of the 19 kDa LvVago1 protein in both inclusion bodies and the soluble fraction specifically in BL21(DE3)-CodonPlus (Figure 2B). Conversely, BL21(DE3) and Rosetta (DE3) exhibited no detectable LvVago1 expression (Figure 2A and C). Consequently, BL21(DE3)-CodonPlus was identified as the optimal strain for subsequent LvVago1 protein expression investigations. The next phase of this research will involve optimizing binding buffers to enhance the efficiency of LvVago1 protein purification.

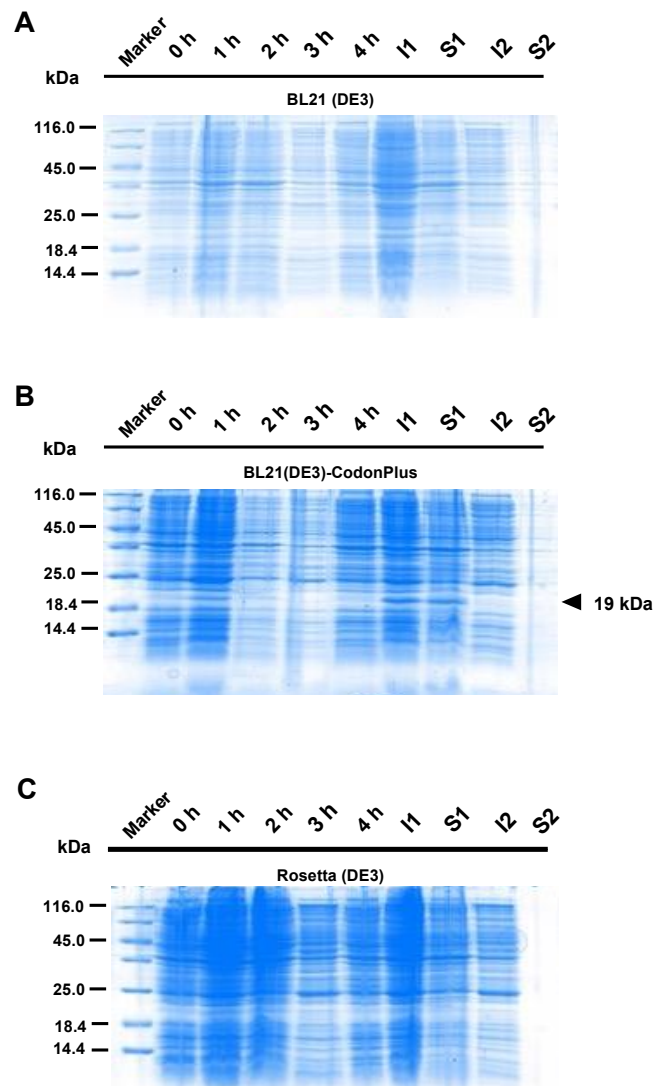


Figure 2 The SDS-PAGE analysis of recombinant LvVago1 expression. The expected molecular mass for recombinant LvVago1 is 19 kDa. (1-4h: after adding 1 mM IPTG, I1 and I2: inclusion bodies, S1 and S2: soluble fraction)

Purification and Immunoblotting of Recombinant LvVago1 Protein

To optimize binding buffers for enhanced LvVago1 protein purification, recombinant LvVago1 was expressed in an E. coli system, and the inclusion body proteins were purified using Ni-NTA agarose beads (GoldBio). The purified LvVago1, with an expected size of approximately 19 kDa (Figure 2B), was eluted using buffers containing either 6 M urea or 1% SDS in 1x PBS (pH 7.4) with various imidazole concentrations (20 mM, 50 mM, 100 mM, and 150 mM). It was observed that the elution buffer with 6 M urea and 150 mM imidazole in 1x PBS (pH 7.4) effectively eluted the LvVago1 protein, as indicated by the bands on the Western Blot (Figure 3B). In contrast, the buffer with 1% SDS in 1x PBS (pH 7.4) failed to elute LvVago1 protein at all tested imidazole concentrations, as shown by the absence of bands (Figure 3A).

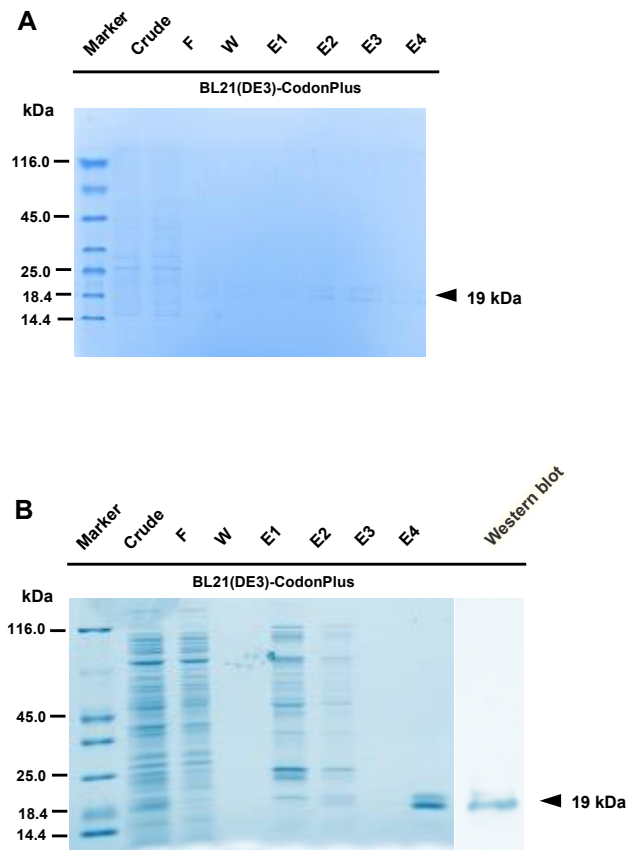


Figure 3 Protein purification with Ni-NTA agarose resin and Western blot analysis of expressed LvVago1 using mouse anti-His-Tag monoclonal antibody (ABclonal) with HRP-conjugated goat anti-mouse IgG (ABclonal). The predicted weight of recombinant LvVago1 is 19 kDa. (F: flow-through, W: wash, E1–E4: different imidazole concentrations including 20mM, 50mM, 100mM, and 150mM of elution.)

Discussions

The successful cloning of the LvVago1 gene into the pET22b vector was confirmed through restriction enzyme digestion and PCR colony screening, demonstrating the efficacy of the cloning protocol (Figure 1). The primers were designed with NcoI and BamHI restriction sites, which facilitated the directional cloning of LvVago1, ensuring the gene was inserted correctly into the vector. This precision in cloning is critical for maintaining the integrity of the gene sequence and ensuring successful downstream applications. The inclusion of a His-tag in the reverse primer was a strategic choice to aid in the purification process, highlighting the importance of thoughtful primer design in molecular cloning.

Expression analysis in various *E. coli* strains identified BL21(DE3)-CodonPlus as the most suitable host for the production of the 19 kDa LvVago1 protein (Figure 2). This strain, optimized for rare codon usage, likely enhanced the translation efficiency of LvVago1, which was not achieved in BL21(DE3) and Rosetta (DE3). The significant expression of LvVago1 in BL21(DE3)-CodonPlus emphasizes the importance of host strain selection



in recombinant protein expression. Host strains that are engineered to enhance the expression of proteins with rare codons can significantly improve yield and solubility, which are critical factors for successful protein production.

The purification of LvVago1 was optimized using Ni-NTA agarose beads, leveraging the His-tag for affinity purification (Figure 3). The study evaluated different binding buffers, with the buffer containing 6 M urea and 150 mM imidazole proving most effective for eluting the LvVago1 protein, as verified by Western blot analysis. Buffers containing 1% SDS failed to elute the protein, indicating that urea was essential for maintaining the solubility and stability of LvVago1 during purification. This finding underscores the importance of optimizing buffer compositions in purification protocols, particularly for proteins that form inclusion bodies. Effective buffer selection is crucial for maximizing the recovery and purity of recombinant proteins.

Conclusions

In summary, this study successfully cloned, expressed, and purified the LvVago1 protein, demonstrating that the BL21(DE3)-CodonPlus strain is the optimal host for its production. The use of strategic primer design, incorporating NcoI and BamHI restriction sites and a His-tag, facilitated accurate cloning and efficient purification via Ni-NTA agarose affinity chromatography. Optimization of binding buffers revealed that 6 M urea with 150 mM imidazole was most effective in eluting the recombinant protein, highlighting the critical role of buffer composition in purification protocols. These findings provide a robust methodological framework for future research on the functional characterization of LvVago1 and its role in invertebrate immune responses, potentially informing new approaches in biotechnology.

Acknowledgements

This work was supported by (i) Suranaree University of Technology (SUT), (ii) Thailand Science Research and Innovation (TSRI), and (iii) National Science, Research, and Innovation Fund (NSRF) (grant number 195581)

References

- Bradford, M. M. (1976). A rapid and sensitive method for the quantitation of microgram quantities of protein utilizing the principle of protein-dye binding. *Analytical biochemistry*, 72(1-2), 248-254.
- Chen, K., Li, E., Gan, L., Wang, X., Xu, C., Lin, H., Qin, J. G., & Chen, L. (2014). Growth and lipid metabolism of the pacific white shrimp *Litopenaeus vannamei* at different salinities. *Journal of Shellfish Research*, 33(3), 825-832.
- He, Y., Wang, S., Zhang, J., Zhang, X., Sun, F., He, B., & Liu, X. (2019). Integrative and conjugative elements-positive *Vibrio parahaemolyticus* isolated from aquaculture shrimp in Jiangsu, China. *Frontiers in microbiology*, 10, 1574.
- Li, F., & Xiang, J. (2013). Signaling pathways regulating innate immune responses in shrimp. *Fish & shellfish immunology*, 34(4), 973-980.



- Liu, Y., Hou, F., He, S., Qian, Z., Wang, X., Mao, A., Sun, C., & Liu, X. (2014). Identification, characterization and functional analysis of a serine protease inhibitor (Lvserpin) from the Pacific white shrimp, *Litopenaeus vannamei*. *Developmental & Comparative Immunology*, 43(1), 35-46.
- Ma, T. H.-T., Benzie, J. A., He, J.-G., & Chan, S.-M. (2008). PmLT, a C-type lectin specific to hepatopancreas is involved in the innate defense of the shrimp *Penaeus monodon*. *Journal of invertebrate pathology*, 99(3), 332-341.
- Shi, B., Xu, F., Zhou, Q., Regan, M. K., Betancor, M. B., Tocher, D. R., Sun, M., Meng, F., Jiao, L., & Jin, M. (2021). Dietary organic zinc promotes growth, immune response and antioxidant capacity by modulating zinc signaling in juvenile Pacific white shrimp (*Litopenaeus vannamei*). *Aquaculture Reports*, 19, 100638.



Production and Purification Recombinant sVP28 Protein for Antibody Generation

¹ Seabkongseng, T. , ¹ Limkul, S. , ¹ Aunkam, P. , ¹ Suwantit, R. , ¹ Phiwthong, T. and ^{1*} Boonchuen, P.

¹ School of Biotechnology, Institute of Agricultural Technology, Suranaree University of Technology, Nakhon Ratchasima, Thailand 30000

*Corresponding author: pakpoom.b@sut.ac.th

Abstract

sVP28 is a part of the VP28 gene found in a circular RNA derived from White Spot Syndrome Virus (WSSV), which is one of pathogens that affects the aquaculture of shrimp globally. sVP28 is found to play an important role in the shrimp immune response. According to previous studies, VP28 protein is one of WSSV capsid proteins being utilized to produce antibodies able to detect the infection of WSSV in shrimp. However, no report has established the antibody against the sVP28 protein. Therefore, this study wanted to produce and purify recombinant sVP28 protein to generate antibodies that are specific to the sVP28 protein. The protein was overexpressed using bacteria, which was then purified using the protein purification from polyacrylamide gel instead and the highly purified protein was attainable via this technique. The purified protein can, hence, be used to generate antibodies, which are able to thoroughly examine the role of the sVP28 protein, as well as develop new methods to prevent and treat diseases caused by WSSV, which could reduce its impact on the shrimp farming industry.

Keywords: sVP28, Recombinant protein, affinity chromatography, protein purification

Introduction

White Spot Syndrome Virus (WSSV) is a significant pathogen in the global aquaculture industry, particularly affecting shrimp farming (Lightner, 2011). The economic impact of WSSV outbreaks can be devastating, with shrimp mortality rates reaching up to 100% within 3 to 5 days post-infection. WSSV is a large, enveloped double-stranded DNA virus associated with the genus *Whispovirus* within the virus family *Nimaviridae*. It has a wide host range among crustaceans (Pradeep et al., 2012; Sánchez-Paz, 2010).

One of the viral proteins, VP28, is a major structural protein that has been extensively studied for its role in the virus's infection mechanism and its potential as a target for diagnostic tools and vaccines (van Hulten et al., 2001). Previous studies have demonstrated that VP28 can induce protective immunity in shrimp. The recombinant VP28 expressed in insect cells conferred significant protection against WSSV in shrimp (Kumar et al., 2008). Furthermore, silencing of the VP28 gene using RNA interference (RNAi) has shown promise in reducing viral loads and improving survival rates in infected shrimp (Westenberg et al., 2005). Antibodies against the VP28 protein can effectively detect WSSV infections in shrimp, facilitating early diagnosis and management of the disease (Chaivisuthangkura et al., 2004; Hou et al., 2011). sVP28 is a part of the VP28 gene found in a circular RNA derived from the WSSV, plays an important role in the shrimp's immune response. Despite its potential significance, there has been no report to date of antibodies developed specifically against



the sVP28 protein. The availability of sVP28-specific antibodies will facilitate in-depth studies on the role of sVP28 in the shrimp immune response and its interaction with WSSV. Additionally, these antibodies could lead to the development of novel diagnostic methods and therapeutic interventions aimed at reducing the impact of WSSV on shrimp farming.

This research aimed to produce and purify the recombinant sVP28 protein to generate antibodies specifically targeting the sVP28 protein. To achieve this, the protein was overexpressed in bacterial systems. Following overexpression, the protein underwent a purification process using polyacrylamide gel electrophoresis. This method proved effective in isolating the sVP28 protein to a high degree of purity. The successfully purified sVP28 protein can be utilized to produce antibodies. These antibodies will play a crucial role in detailed studies of the sVP28 protein's function. Additionally, they can be instrumental in the development of novel strategies for the prevention and treatment of diseases caused by the White Spot Syndrome Virus (WSSV).

Materials and Methods

Expression of recombinant sVP28 protein

To produce the sVP28 protein, the expression vector pET21a+/sVP28 was transformed into *Escherichia coli* BL21 (DE3)-CodonPlus and *Escherichia coli* Rosetta (DE3) strain, which served as the host strain for protein synthesis. These transformed cells were then cultured in an LB medium until they reached an optical density (OD₆₀₀) between 0.4 and 0.6, which is optimal for protein expression. 1 M isopropyl β -D-1-thiogalactopyranoside (IPTG) was added to a final concentration of 1 mM, the induction was carried out under controlled conditions, maintaining the cultures at 30°C and shaking at 250 rpm 4 h. After the induction period, the cells were collected by centrifugation to separate them from the culture medium. The harvested cells were then stored at -80°C to preserve the protein and maintain the cells' integrity for further downstream processing and analysis

Purification of recombinant sVP28 protein

To purify the recombinant protein, cells were harvested and resuspended in binding buffer (1XPBS pH 7.4). The cells were then disrupted using sonication, and the inclusion bodies were harvested and dissolved in binding buffer supplemented with 1XPBS pH 7.4. The recombinant sVP28 proteins were subsequently purified using a Ni-NTA agarose bead column (GoldBio). The protein was eluted using elution buffer containing different concentrations of imidazole (50 mM, 150 mM, and 250 mM). Protein purity was assessed using SDS-PAGE.

Recombinant protein production of sVP28

The purification process of the recombinant sVP28 protein involved initial observation using SDS-PAGE. After the electrophoresis, the protein bands of interest were carefully cut out from the gel using a razor blade. These excised gel pieces were then washed three times, each for 5 minutes of 1XPBS pH 7.4. The gel slices were then finely chopped into small pieces of 2–5 mm. Subsequently, 1X PBS pH 7.4, containing 0.1% SDS, was added to the gel fragments to achieve a buffer-to-gel volume ratio of about 2:1. The mixture was then sonicated for 3 minutes in an ice bath. The sonicated gel fragments were separated from the extraction



buffer, the sample was applied to a filter column and centrifuged at 500g for 10 minutes. The purity of the isolated protein was again assessed using SDS-PAGE.

Next, the recombinant sVP28 proteins were purified using a Ni-NTA agarose column (GoldBio). The proteins were subjected to washing and elution steps, first with 50 mM imidazole in PBS pH 7.4 and then with 250 mM imidazole in 1XPBS pH 7.4, respectively. The fractions containing the recombinant proteins were combined and subjected to dialysis against a solution of 1XPBS pH 7.4. The protein concentration was then determined using the BCA method.

Confirmation and detection of sVP28 protein

To confirm and detect the sVP28 protein, the recombinant sVP28 protein was first separated using SDS-PAGE and subsequently transferred to a membrane. The membrane was then blocked with 5% skim milk in 1X PBS containing 0.1% Tween 20 for 1 hour at room temperature to prevent non-specific binding. Following this, the membrane was incubated for 1 hour at room temperature with a VP28 antibody (diluted 1:10,000), prepared according to the method described by Tsai et al. (2006) (Tsai et al., 2006). The membrane was washed three times with 1X PBS with 0.1% Tween 20. Next, an HRP-conjugated goat anti-rabbit IgG (diluted 1:10,000) from Abbkine was used as the secondary antibody, followed by three additional washes with 1X PBS containing 0.1% Tween 20. The chemiluminescent signal was detected using the Amersham ECL Prime Western blotting detection reagent substrate from Cytiva.

Results

Expression and Extraction of recombinant sVP28 protein

To produce recombinant sVP28 protein, we utilized the *E. coli* expression system with strains including *E. coli* BL21(DE3)-CodonPlus and *E. coli* BL21 Rosetta (DE3). The protein was successfully overexpressed in *E. coli* BL21(DE3)-CodonPlus, demonstrating the expected size of approximately 19.5 kDa (Figure 1). However, consistent overexpression was not achieved in *E. coli* BL21 Rosetta (DE3). Following expression, the recombinant sVP28 proteins in *E. coli* BL21(DE3)-CodonPlus were subsequently purified using a Ni-NTA agarose bead column (GoldBio).

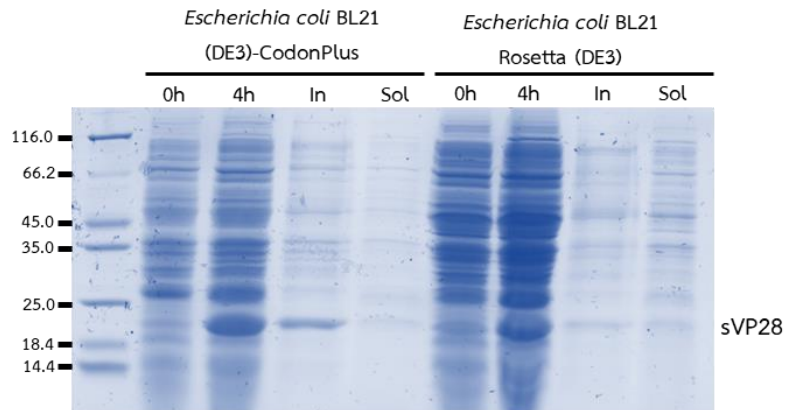


Figure 1 The expression of recombinant sVP28 protein. The expected size of approximately 19.5 kDa. (0h: befor adding 1 mM IPTG, 4h: after adding 1 mM IPTG, In: inclusion bodies, Sol: soluble)

Protein Purification from affinity chromatography

For the purification of recombinant sVP28 protein, *E. coli* BL21(DE3)-CodonPlus was employed for protein expression. Initially, the inclusion bodies were purified using a Ni-NTA agarose bead column (GoldBio). The protein was initially eluted using elution buffers containing different concentrations of imidazole (50 mM, 150 mM, and 250 mM) (Figure 2). However, proteins eluted from the column effectively only at 250 mM imidazole, suggesting the presence of some contaminants. Further purification was carried out using polyacrylamide gels via sonication extraction.

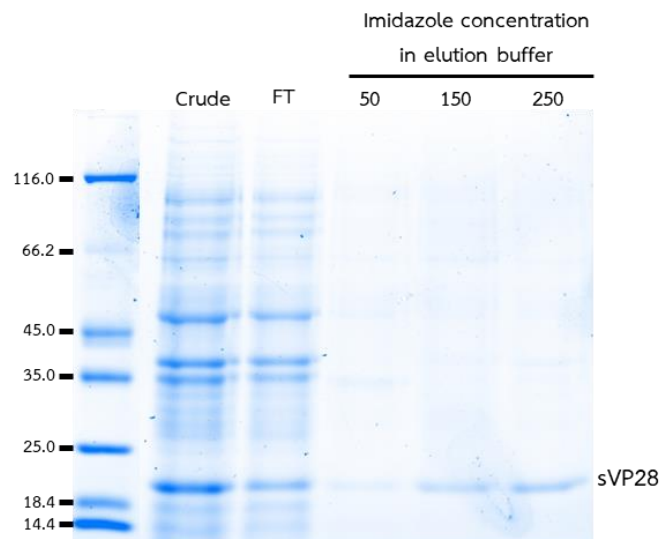


Figure 2 Recombinant sVP28 protein using Ni-NTA agarose bead column (GoldBio). The expected size of approximately 19.5 kDa. (F: flow-throug, 50-250: imidazole concentration in elution buffer)

Purification from Polyacrylamide Gels by Sonication Extraction and Confirmation of sVP28 protein

To confirmation and detection for enhanced recombinant sVP28 protein, protein was purified from polyacrylamide gels using sonication extraction, indicating some impurities persisted (Figure 3A). This

necessitated further purification using Ni-NTA agarose bead column (GoldBio) led to (Figure 3B), where only a characteristic molecular weight band of 19.5 kDa was observed on SDS-PAGE analysis. The Western Blot analysis of recombinant sVP28 protein shows two major immunoreactive bands with appare 19.5 kDa.

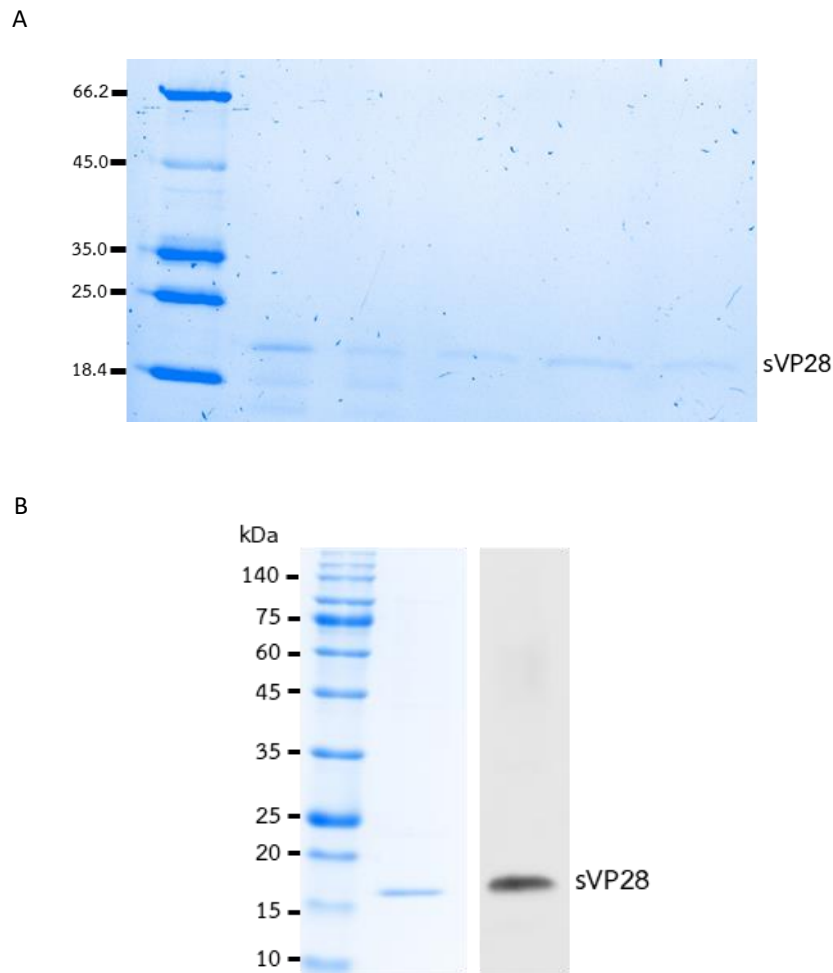


Figure 3 Protein purification from Polyacrylamide Gels by Sonication Extraction and Western blot analysis of recombinant sVP28 protein. (A) The purified sVP28 proteins extracted from polyacrylamide gels using sonication were analyzed by SDS-PAGE. (B) Western blot analysis confirmed the presence of a band corresponding to sVP28.

Discussion

To produce and purify recombinant sVP28 protein from White Spot Syndrome Virus (WSSV) to generate specific antibodies, a significant step towards understanding its role in shrimp immunity and developing diagnostic and therapeutic tools against WSSV. The successful expression and purification of sVP28 were achieved using both affinity chromatography and polyacrylamide gel extraction techniques, confirming its purity and specificity through SDS-PAGE and Western blot analysis.



The expression of sVP28 in *Escherichia coli* strains BL21 (DE3)-CodonPlus and Rosetta (DE3) yielded differing results, with optimal expression observed in *E. coli* BL21 (DE3)-CodonPlus (Figure 1). This variation underscores the importance of host strain selection in recombinant protein expression, aligning with previous studies that highlighted the influence of host genetic background on protein yield and quality (Shevchenko et al., 1996).

Affinity chromatography using Ni-NTA agarose beads initially provided purification, although at 250 mM imidazole concentration (Figure 2), indicating some impurities persisted. This necessitated further purification using polyacrylamide gel extraction via sonication, which improved purity as evidenced by the absence of non-specific bands on SDS-PAGE (Figure 3A-B). The use of sonication extraction from polyacrylamide gels has been reported as effective in isolating proteins from complex mixtures (Retamal et al., 1999; Shevchenko et al., 1996), supporting its application in this study. Western blot analysis confirmed the presence of sVP28 protein at approximately 19.5 kDa, consistent with the expected molecular weight, validating the purification methods used. The successful generation of antibodies specific to sVP28 opens avenues for exploring its immunological function in shrimp, potentially enhancing diagnostic accuracy and therapeutic efficacy against WSSV infections in aquaculture.

This research contributes to the broader understanding of WSSV pathogenesis and host immune response mechanisms, offering insights into how sVP28 interacts with shrimp immunity. Future studies could focus on elucidating the precise role of sVP28 in WSSV infection dynamics and evaluating its potential as a vaccine candidate or diagnostic marker.

Conclusions

In conclusion, this study successfully expressed and purified recombinant sVP8 protein from *Escherichia coli* using both affinity chromatography and polyacrylamide gel extraction techniques. The results indicate that polyacrylamide gel extraction techniques demonstrating its purity and specificity as evidenced by confirmed through SDS-PAGE and Western blot analysis. This achievement lays the groundwork for further research into the role of sVP28 in shrimp immune response and its potential applications in diagnostics and therapeutics for WSSV. By generating antibodies specific to sVP28, this study opens avenues for developing novel strategies to mitigate the impact of WSSV outbreaks on shrimp farming.

Acknowledgements

This research was supported by (i) Suranaree University of Technology (SUT), (ii) Thailand Science Research and Innovation (TSRI), and (iii) National Science, Research, and Innovation Fund (NSRF) (grant number 195581)

References

Chaivisuthangkura, P., Tangkhabuanbutra, J., Longyant, S., Sithigorngul, W., Rukpratanporn, S., Menasveta, P., & Sithigorngul, P. (2004). Monoclonal antibodies against a truncated viral envelope protein (VP28) can detect white spot syndrome virus (WSSV) infections in shrimp. *ScienceAsia*, 30, 359-363.



- Hou, C.-L., Cao, Y., Xie, R.-h., Wang, Y.-z., & Du, H.-h. (2011). Characterization and diagnostic use of a monoclonal antibody for VP28 envelope protein of white spot syndrome virus. *Virologica Sinica*, *26*, 260-266.
- Kumar, R., Mukherjee, S., Ranjan, R., & Nayak, S. (2008). Enhanced innate immune parameters in *Labeo rohita* (Ham.) following oral administration of *Bacillus subtilis*. *Fish & Shellfish Immunology*, *24*(2), 168-172.
- Lightner, D. V. (2011, Jan). Virus diseases of farmed shrimp in the Western Hemisphere (the Americas): a review. *J Invertebr Pathol*, *106*(1), 110-130. <https://doi.org/10.1016/j.jip.2010.09.012>
- Pradeep, B., Rai, P., Mohan, S. A., Shekhar, M. S., & Karunasagar, I. (2012). Biology, host range, pathogenesis and diagnosis of white spot syndrome virus. *Indian Journal of Virology*, *23*, 161-174.
- Retamal, C. A., Thiebaut, P., & Alves, E. W. (1999). Protein purification from polyacrylamide gels by sonication extraction. *Analytical Biochemistry*, *268*(1), 15-20.
- Sánchez-Paz, A. (2010). White spot syndrome virus: an overview on an emergent concern. *Veterinary research*, *41*(6).
- Shevchenko, A., Wilm, M., Vorm, O., & Mann, M. (1996). Mass spectrometric sequencing of proteins from silver-stained polyacrylamide gels. *Analytical chemistry*, *68*(5), 850-858.
- Tsai, J.-M., Wang, H.-C., Leu, J.-H., Wang, A. H.-J., Zhuang, Y., Walker, P. J., Kou, G.-H., & Lo, C.-F. (2006). Identification of the nucleocapsid, tegument, and envelope proteins of the shrimp white spot syndrome virus virion. *Journal of virology*, *80*(6), 3021-3029.
- van Hulten, M. C., Witteveldt, J., Snippe, M., & Vlak, J. M. (2001). White spot syndrome virus envelope protein VP28 is involved in the systemic infection of shrimp. *Virology*, *285*(2), 228-233.
- Westenberg, M., Heinhuis, B., Zuidema, D., & Vlak, J. M. (2005). siRNA injection induces sequence-independent protection in *Penaeus monodon* against white spot syndrome virus. *Virus Research*, *114*(1-2), 133-139.